Diversification of the African legless skinks in the subfamily Acontinae (Family Scincidae)

Zhongning Zhao [a,b,*], Werner Conradie [c,d], Darren W. Pietersen [e], Adriaan Jordaan [a], Gary Nicolau [f], Shelley Edwards [f,] Stephanus Riekert g, Neil Heideman [a]

[a]Department of Zoology and Entomology, University of the Free State, Bloemfontein, South Africa
[b]Department of Genetics, University of the Free State, Bloemfontein, South Africa
[c]Port Elizabeth Museum (Bayworld), P.O. Box 13147, Humewood, Port Elizabeth 6013, South Africa
[d]Department of Nature Conservation Management, Natural Resource Science and Management Cluster, Faculty of Science, George Campus, Nelson Mandela University, George, South Africa
[e]Department of Zoology and Entomology, University of Pretoria, Private Bag X20, Hatfield 0028, South Africa
[f]Zoology & Entomology Molecular Lab, Department of Zoology and Entomology, Rhodes University, Makhanda, South Africa
[g]Department of Information and Communication Technology Services, University of the Free State, Bloemfontein, South Africa

* Corresponding author at: Department of Zoology and Entomology, University of the Free State, Bloemfontein, South Africa. Email: orochi19851020@yahoo.com

Highlights

- A large-scale study investigating the complex genetic structure, species boundaries, evolutionary relationships, and diversification among all the species in the subfamily Acontinae.
- The subfamily Acontinae is an African group of legless skinks which consists of multiple species complexes.
- This study resolved many long-standing phylogenetic enigmas and clarified many blurry species boundaries within the subfamily Acontinae in general and within its species complexes.
- Lineage diversification is associated with Miocene climatic oscillations, epeirogenic uplift, expansion of open habitats, variable rainfall patterns, and the presence of the warm Agulhas Current since the early Miocene, as well as their co-effects.
- Possible "ghost introgression" and interspecies gene flow was detected in the subfamily Acontinae.

Graphical abstract

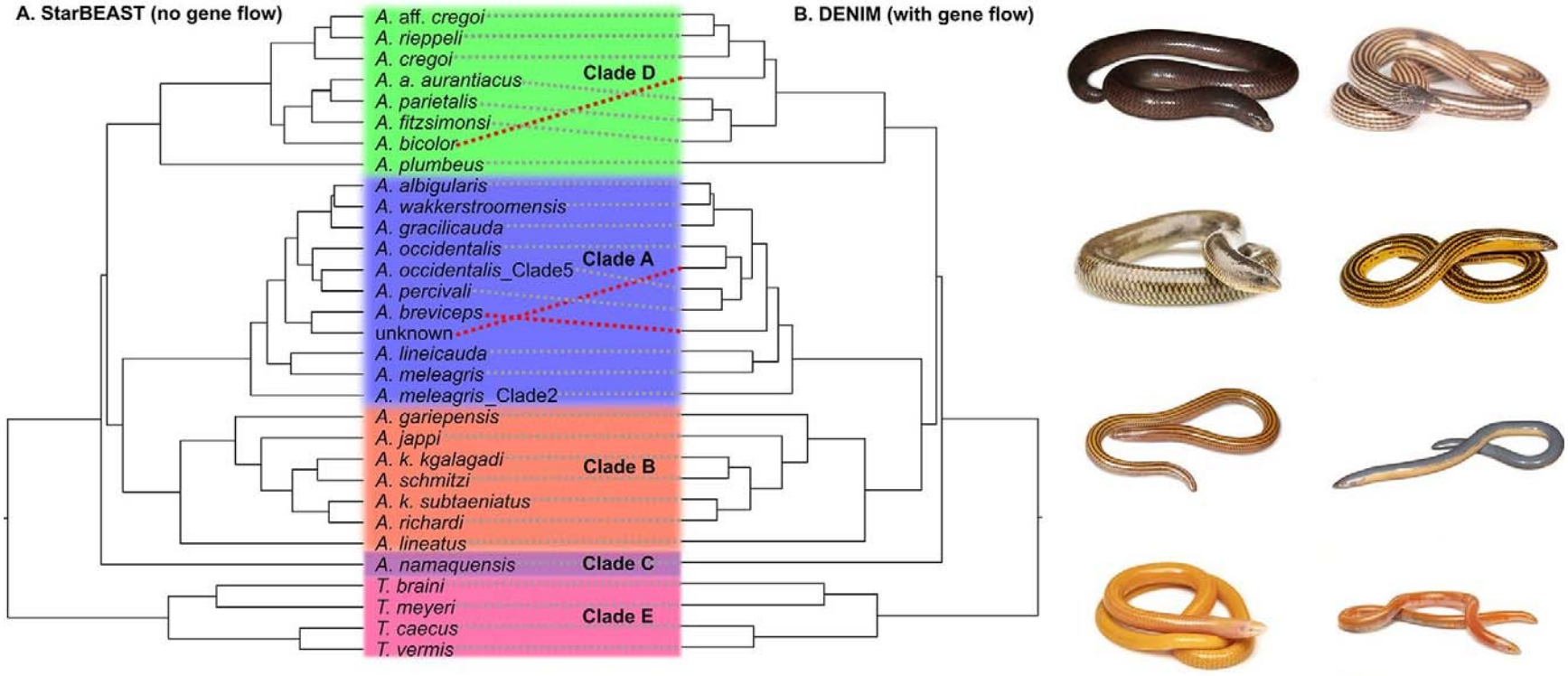

Abstract

Cladogenic diversification is often explained by referring to climatic oscillations and geomorphic shifts that cause allopatric speciation. In this regard, southern Africa retains a high level of landscape heterogeneity in vegetation, geology, and rainfall patterns. The legless skink subfamily Acontinae occurs broadly across the southern African subcontinent and therefore provides an ideal model group for investigating biogeographic patterns associated with the region. A robust phylogenetic study of the Acontinae with comprehensive coverage and adequate sampling of each taxon has been lacking up until now, resulting in unresolved questions regarding the subfamily's biogeography and evolution. In this study, we used multi-locus genetic markers (three mitochondrial and two nuclear) with comprehensive taxon coverage (all currently recognized Acontinae species) and adequate sampling (multiple specimens for most taxa) of each taxon to infer a phylogeny for the subfamily. The phylogeny retrieved four well-supported clades in *Acontias* and supported the monophyly of *Typhlosaurus*. Following the General Lineage Concept (GLC), many long-standing phylogenetic enigmas within *Acontias occidentalis* and the *A. kgalagadi*, *A. lineatus* and *A. meleagris* species complexes, and within *Typhlosaurus* were resolved. Our species delimitation analyses suggest the existence of hidden taxa in the *A. occidentalis*, *A. cregoi* and *A. meleagris* species groups, but also suggest that some currently recognized species in the *A. lineatus* and *A. meleagris* species groups, and within *Typhlosaurus*, should be synonymised. We also possibly encountered "ghost introgression" in *A. occidentalis*. Our inferred species tree revealed a signal of gene flow, which implies possible cross-over in some groups. Fossil evidence calibration dating results showed that the divergence between *Typhlosaurus* and *Acontias* was likely influenced by cooling and increasing aridity along the southwest coast in the mid-Oligocene caused by the opening of the Drake Passage. Further cladogenesis observed in *Typhlosaurus* and *Acontias* was likely influenced by Miocene cooling, expansion of open habitat, uplifting of the eastern Great Escarpment (GE), and variation in rainfall patterns, together with the effect of the warm Agulhas Current since the early Miocene, the development of the cold Benguela Current since the late Miocene, and their co-effects. The biogeographic pattern of the Acontinae bears close resemblance to that of other herpetofauna (e.g., rain frogs and African vipers) in southern Africa.

Keywords: Divergence dating; 'ghost introgression'; Miocene cooling; Open habitat; Species delimitation; Uplift

1. Introduction

Two main goals of systematic biology are using the reconstruction of phylogenies: (1) to demarcate species boundaries and unravel the systematic relationships among taxa, and (2) to address evolutionary or biogeographic questions (Wiens, 2007). In recent decades, modern systematics and taxonomy advocates have used the General Lineage Concept (GLC) to attempt to solve the conflicts among different species concepts (de Queiroz, 2005, de Queiroz, 2007). Under the GLC, given enough time, metapopulations diverge into several independent evolutionary lineages. The GLC aims to move away from recognizing "species" on the basis of a single criterion (e.g., morphology, genetics, ecology, monophyly) to the recognition of evolutionary distinct lineages that also take into account temporal and spatial scales (de

Queiroz, 2007). The GLC has been widely regarded as a useful, practical, and operational blueprint for species delimitation given its inclusive nature in drawing on multiple criteria (Reeves and Richards, 2011). Molecular markers are among the most practical and informative diagnostic tools for identifying plausible general lineages. Putative taxonomic units retrieved from these delimitation methods may represent populations, species, or a combination of the two. To establish proper Operational Taxonomic Units (OTUs) for conservation management, it is however important to also consider other evidence, such as ecology, recognition mechanisms, reproductive isolation, acoustic features, and morphology (Sukumaran and Knowles, 2017). However, speciation is regarded as a continuous process (Stankowski and Ravinet, 2021), and ongoing gene flow between different lineages can result from hybridization or introgression as a result of incomplete reproductive isolation (Conflitti et al., 2014). These gene flow effects may homogenize the diverging pattern between closely related groups (Petit and Excoffier, 2009), making the recovery of true genealogies quite challenging. This is particularly true with the existence of Incomplete Lineage Sorting (ILS) resulting from gene tree–species tree discordance (Degnan and Rosenberg, 2006). In this regard, the Bayesian Multispecies Coalescent (MSC) model allows for the inference of independent species trees from multiple unlinked loci to address the issue of gene tree-species tree discordance (Rannala and Yang, 2003).

Biogeography aims to investigate the geographic patterns of organisms and the factors that determine those patterns (King et al., 2006). To understand contemporary biogeographic patterns, it is essential to be familiar with the evolutionary history of organisms, and the relevant background information of palaeogeography and palaeoclimatology (Tolley et al., 2008). Historical processes, such as climate oscillations and topographical shifts, play fundamental roles in shaping diversification patterns and changing the genetic structure of diverse populations (Hewitt, 2000, Tolley et al., 2008, Portik et al., 2011, Gray et al., 2019, Zhao et al., 2020a). Physical vicariant barriers (e.g., mountains or rivers) can block gene flow between populations and result in allopatric isolation, which is a fundamental driving force of speciation (Fitzpatrick et al., 2009). In theory, the cold phase of background climates (e.g., cooling events, glaciation, etc.) can result in populations contracting into subpopulations along refugia thereby facilitating allopatric speciation processes. During the warm phase, glaciers retract, leading to population expansion, dispersal, and recolonization (Hewitt, 1996, Hewitt, 1999, Hewitt, 2004). To understand how these processes influence diversification in certain regions, it is crucial to clarify geographic distribution and boundaries between populations or closely related species (Barlow et al., 2013). Geographic patterns of lineage divergence resulting from allopatric speciation are usually caused by the combined effects of geographic and ecological barriers (Nielsen et al., 2018, Gray et al., 2019, Butler et al., 2023).

The high diversity of reptiles and amphibians in southern Africa has broadly been attributed to paleoclimatic oscillations and geomorphological shifts (Tolley et al., 2008, Barlow et al., 2013, Engelbrecht et al., 2013, da Silva and Tolley, 2017, Nielsen et al., 2018, Busschau et al., 2019, Busschau et al., 2022, Zhao et al., 2020a;). These climatic and geomorphological changes would have resulted in large-scale landscape heterogeneity in vegetation, geology, and rainfall patterns, which would have been strong drivers of cladogenesis (Cowling et al., 2009). The opening of the Drake Passage caused the cold Benguela Current (Fig. 1) to flow northward along the west coast of southern Africa (Feakins and deMenocal, 2010), resulting in the aridity of southern Africa progressively increasing (Burke and Gunnell, 2008). Besides this, the formation of the Antarctic ice sheet since the early Oligocene resulted in global cooling (Zachos et al., 2001). This cooling, together with the gradual aridification, possibly contributed to lineage diversification and the separation of ancestral lineages into distinct geographic areas

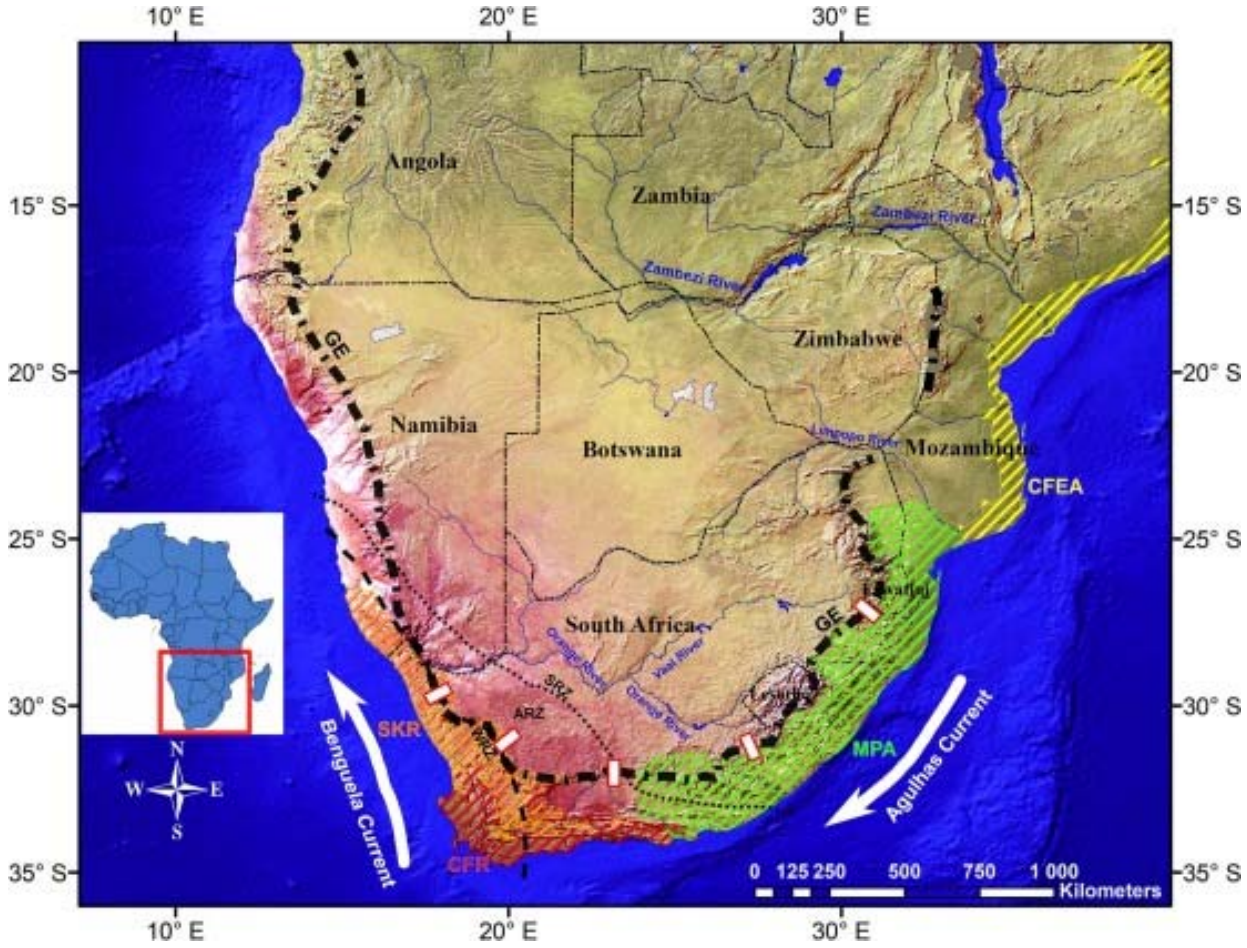

Fig. 1. Southern Africa, highlighting the relevant global biodiversity hotspots: Cape Floristic Region (CFR, red), Succulent Karoo Region (SKR, orange), Maputaland-Pondoland-Albany (MPA, green), and Coastal Forests of East Africa (CFEA, yellow). Some biogeographically relevant features are indicated, including the Great Escarpment (GE), major rivers (in blue), rainfall zones (winter rainfall zone = WRZ, summer rainfall zone = SRZ, and aseasonal rainfall zones = ARZ), and ocean currents (Benguela and Agulhas). White boxes with red margins represent open corridors through the GE mentioned by Clark et al. (2011).

(Zhao et al., 2020a). Global cooling from the mid-to-late Miocene, ~15–10 Ma (Zachos et al., 2001) initiated widespread aridification and the expansion of open arid habitats and contraction of closed mesic habitats, which in turn influenced the cladogenic radiations of organisms associated with these habitats (Hewitt, 1996, Hewitt, 1999, Hewitt, 2004, Jansson and Dynesius, 2002, deMenocal, 2004). By the late Miocene, the development of the cold Benguela Current greatly intensified aridification of the western region and established seasonal rainfall patterns (Fig. 1) over southern Africa (Rommerskirchen et al., 2011, Hoetzel et al., 2015, Hoffmann et al., 2015, Neumann and Bamford, 2015), which may have also caused retracting of refugia, possibly leading to diversification. The rainfall patterns demarcated southern Africa into three zones (Fig. 1): a Winter Rainfall Zone (WRZ), an Aseasonal Rainfall Zone (ARZ), and a Summer Rainfall Zone (SRZ) (Chase and Meadows, 2007). Comparative biogeography revealed that the unique southern African rainfall pattern may have influenced the diversification patterns and genetic structuring of the herpetofauna in southern Africa (Myburgh and Daniels, 2022), including rain frogs (genus *Breviceps*; Nielsen et al., 2018), the clicking stream frog (*Strongylopus grayii*, Tolley et al., 2010), the western rock skink (*Trachylepis sulcata*; Portik et al., 2011), the angulate tortoise (*Chersina angulata*; Spitzweg et al., 2020), and the tent tortoise species complex (*Psammobates tentorius*; Zhao et al., 2020a). Along the east coast of South Africa, the warm Agulhas Current and uplifting of the Great Escarpment (GE; Fig. 1) established a rain shadow effect, contributing to the aridification of the interior plateau while maintaining a moist subtropical climate along the eastern escarpment (Sepulchre et al., 2006, Neumann and Bamford, 2015). The GE also serves as an important refugium and a significant geographic barrier shaping biogeographic patterns of diverse organisms in southern Africa (Clark et al., 2011). Furthermore, the periodic climatic cycles in response to Milankovitch forces caused glaciers to wax and wane during the Pliocene and Pleistocene epochs (Fedorov et al., 2006), which substantially affected speciation and geographic distributions worldwide (Hewitt, 2000). Reptile diversity is comparatively high in southern Africa (Branch, 1998, Branch, 1999), with the majority of cladogenic events in several taxa being linked to climatic and topographic changes during the Plio-Pleistocene period (deMenocal, 2004, Tolley et al., 2014). Climatic cooling has also influenced diversification in fossorial snake species (Portillo et al., 2018, Portillo et al., 2019, Busschau et al., 2020). Lastly, the gradual intensification of vegetation shifting from C3 photosynthetic plants (forest and thicket) to C4 plants (savanna and grasses) resulted in the expansion of open habitats in southern Africa since the mid-late Miocene (Cerling et al., 1997). This open habitat expansion process is believed to be a driver shaping allopatric diversification in many African reptile species (Medina et al., 2016, Nielsen et al., 2018, Barlow et al., 2019, Busschau et al., 2019, Engelbrecht et al., 2020).

There are 36 global biodiversity hotspots that are classified as regions harboring exceptionally high species richness while also suffering considerable habitat loss (Marchese, 2015, Noss et al., 2015). Although these regions cover only 17.3% of the Earth's land surface area, they contain 77% of all endemic plant species and 43% of all endemic vertebrate species (Mittermeier et al., 2011, Williams et al., 2011). There are three globally recognized biodiversity hotspots in southern Africa (Fig. 1): the Cape Floristic Region (CFR), Succulent Karoo (SKR), and the greater Maputaland-Pondoland-Albany hotspot (MPA; Mittermeier et al., 2011, Williams et al., 2011). These hotspots contribute substantially to the high levels of endemism and diversity of southern African reptiles (Branch, 1998, Bates et al., 2014). Of the 401 described terrestrial reptile species in South Africa, Eswatini, and Lesotho, the 267 lizard species exhibit the highest proportion of diversity and endemism (Bates et al., 2014, Tolley et al., 2022).

Many of the fossorial scincine lizards (including *Acontias, Melanoseps, Scelotes*, *Scolecoseps*, and *Typhlosaurus*) in southern Africa are morphologically very conservative (e.g., all have reduced or absent limbs and are fossorial, while some share very similar body shapes and color patterns, largely lacking any distinguishing characteristics), in contrast to high cryptic diversity as revealed by genetic evidence in many of these groups. The taxonomic status in some of these groups have been clarified (Whiting et al., 2003, Daniels et al., 2009, Heideman et al., 2011, Busschau et al., 2017, Conradie et al., 2018, Pietersen et al., 2018, Zhao et al., 2019). The two genera *Acontias* and *Typhlosaurus* of the skink subfamily Acontinae are legless species found mainly in southern Africa (Broadley and Greer, 1969, Branch, 1998, Bates et al., 2014), with only one species (*A. percivali*) occurring solely outside this range (Broadley, 1968, Broadley and Greer, 1969, Wagner et al., 2012). Twenty-six *Acontias* and five *Typhlosaurus* species are currently recognized (Chapple et al., 2021, Uetz et al., 2022), with the species differing greatly in maximum size and body proportions (Broadley, 1968, Broadley and Greer, 1969, Branch, 1998). The distribution range of the Acontinae broadly spans the three biodiversity hotspots in southern Africa (CFR, SKR, and MPA), with one species (*A. percivali*) occurring in the Coastal Forests of Eastern Africa (CFEA).

The taxonomy of the Acontinae remains dubious, particularly in the case of the genus *Acontias*, due to its high phenotypic variation and cryptic speciation resulting from adaptation to similar environmental pressures (Daniels et al., 2009, Engelbrecht et al., 2013, Busschau et al., 2017, Conradie et al., 2018, Pietersen et al., 2018, Zhao et al., 2019). A morphological study by Evlambiou (2021) found that both skull morphometric measurements and meristic data were unable to satisfactorily distinguish the majority of the Acontinae species. Some previous Acontinae phylogenetic studies have been challenged due to their low sample sizes, the use of single gene markers, and insufficient taxon coverage (Daniels et al., 2002, Daniels et al., 2005, Daniels et al., 2006, Lamb et al., 2010). Furthermore, the systematics of certain groups, particularly the *A. meleagris* species complex (including *A. meleagris*, *A. orientalis* and *A. lineicauda*), the slender-bodied West Coast species group (comprising *A. lineatus*, *A. grayi*, *A. litoralis* and *A. tristis*), and *A. occidentalis*, remains unresolved (Daniels et al., 2009, Janse van Vuuren, 2009, Engelbrecht et al., 2013, Busschau et al., 2017). The population genetic structure within each species, and phylogenetic relationships among *A. gariepensis*, *A. jappi*, *A. k. kgalagadi*, *A. k. subtaeniatus*, *A. richardi*, and *A. schmitzi*, also remain unclear due to the lack of sampling. Lastly, the species boundaries and population genetic structure within *Typhlosaurus* is also poorly studied and awaits further investigation. A comprehensive multi-locus dataset that covers all species together with adequate sampling in each species complex and group is critically important for clearly demarcating species boundaries and constructing the full evolutionary picture of the subfamily Acontinae.

Two factors make the Acontinae an excellent model group for studying diversification and historical biogeographic patterns in southern Africa. First, its broad distribution range across southern Africa and parts of eastern Africa, which includes a significant geographic barrier (the GE), means that species occur in both closed forest and open grassland, in four currently recognized biodiversity hotspots (CFR, SKR, MPA, and CFEA), and three regions with different rainfall patterns (WRZ, ARZ, and SRZ). Second, its ecology and morphology are likely to foster allopatric divergence (e.g., the species are highly dependent on their refugia, thus limiting their dispersal ability). Our main goals with this study were to unravel the longstanding systematic puzzle that has plagued this subfamily, clarify the species boundaries, investigate the biogeographic patterns and cladogenic history, and identify potential drivers that could have shaped the diversification of the subfamily Acontinae. To infer its phylogeny, we used a multi-locus dataset with all currently recognized species and adequate sampling at

the population level in most taxa. We used the GLC and reciprocal monophyly as baselines with modern species delimitation techniques to demarcate species boundaries. We used Bayesian MSC model-based species tree inference to address the potential discordance between gene-tree and species-tree results due to ILS. To incorporate gene flow across species and populations under multiple species coalescence theory, we applied both gene flow and non-gene flow models to address the potential influence of hybridization and introgression. We integrated a fossil-calibrated phylogeny together with the known biogeographic information of other herpetofauna to demonstrate how paleoclimatic oscillations and topographic changes may have shaped the diversification and biogeographic patterns in the Acontinae. We postulated: (1) that cryptic diversity exists in the Acontinae, particularly in the biodiversity hotspots; (2) that the majority of the cladogenic events fell into the period between the mid-Miocene to late Miocene when major Miocene cooling events were experienced in southern Africa; (3) that the estimated divergence time between the groups from the interior plateau and coastal side of the GE coincided with the time of the GE uplift, and that the GE played a role in demarcating the biogeographic patterns of the Acontinae; and (4) that the cladogenic pattern in certain groups of the Acontinae matches the demarcated rainfall patterns (WRZ, ARZ and SRZ) and the segregation between open and closed habitats.

2. Materials and methods

2.1. Sample collection, DNA extraction, sequencing and data assembly

Seventy-three (73) new Acontinae specimens were collected from multiple localities in sub-Saharan Africa, representing 21 currently recognized Acontinae taxa (18/26 species of the genus *Acontias*, 3/5 species of the genus *Typhlosaurus*). Taxa were identified using the morphological descriptions provided in primary literature (Broadley, 1968, Broadley and Greer, 1969, Jacobsen, 1987) and guides (Fitzsimons, 1943, Branch, 1998). Liver or muscle tissue was extracted from each specimen and preserved in 96–99% ethanol for subsequent DNA extraction. We generated sequences for three mitochondrial genes (*16S*, *COI*, and *Cyt-b*) and two nuclear genes (*PRLR* and *Rag-1*) for the 73 specimens (Supplementary Table S1). All the new sequences were deposited in NCBI GenBank (Supplementary Table S1). In addition, all available *Acontias* and *Typhlosaurus* DNA sequences (that had sufficient supporting information) were downloaded from GenBank for the same gene regions (Supplementary Tables S1). In total, our study included sequences from all currently recognized Acontinae taxa of the Acontinae (26/26 species of the genus *Acontias*, 5/5 species of the genus *Typhlosaurus*). We used *Trachylepis capensis* and *Trachylepis sechellensis* as outgroup taxa for our non-time calibrated phylogenetic analyses (Supplementary Table S2). For the calibration dating analysis, we used *Scincus scincus*, *Scincopus fasciatus*, *Eumeces schneiderii*, *Eurylepis taeniolata*, *Liopholis whitii*, *Tiliqua* sp., *Cyclodomorphus gerrardii*, *Cyclodomorphus casuarinae*, *Parvoscincus sisoni*, *Ctenotus* sp., *Calyptotis scutirostrum*, *Concinnia ampla*, *Saiphos equalis*, *Sphenomorphus* sp., *Scincella lateralis*, *Tropidophorus berdmorei*, *Trachylepis capensis*, and *Trachylepis sechellensis* as outgroups (Supplementary Tables S2). All alignment files are provided in the Supplementary files (S1–S6).

Total genomic DNA was extracted using a Qiagen DNeasy Blood & Tissue Extraction Kit (Qiagen, Germany) following the manufacturer's protocol. We used Polymerase Chain Reaction (PCR) to sequence three mtDNA and two nDNA loci using the primers listed in Table 1. PCRs were performed using TEMPase Hot Start Master Mix (USAS), following the manufacturers' instructions. Independent temperature gradient tests determined the optimal annealing temperatures for each gene. All PCR reactions were performed in a Bio-Rad T100™

Table 1. Primers used for sequencing mitochondrial and nuclear genes.

Gene name	Primer name	Primer sequence (5′ to 3′)	Primer source	Number of cycles	Annealing temperature (°C)	Extension temperature (°C)
16S	16Sar	CGCCTGTTTATCAAAAACAT	Cunningham et al. (1992)	35	50	72
	16Sbr	CCGGTCTGAACTCAGATCACGT				
COI	COI-LBF	CTGCAGGAGGAGGAGATCCRATMTTRTATCAACA	Lamb et al. (2010)	32	50	68
	COI-LBR	GTCTGGGTAGTCTGAGTATCGTCGTGGTAT				
Cyt-b	CytbR2	GGGTGRAAKGGRATTTTATC	Whiting et al. (2003)	35	50	72
	WWF	AAAYCAYCGTTGTWATTCAACTAC				
Rag-1	None	TCGCTTGAAAAACCACTTCCTGARCT	Lamb et al. (2010)	45	58	68
	None	TCAGCAAAAGCCTTCACTTGAAGC				
PRLR	PRLRf1	GACARYGARGACCAGCAACTRATGCC	Townsend et al. (2008)	45	58	72
	PRLRr3	GACYTTGTGRACTTCYACRTAATCCAT				

Thermal Cycler (Singapore) under the following conditions: an initial 15 min denaturation step at 94 °C, followed by cycles of 60 s of denaturation at 94 °C, 45 s annealing, and 90 s extension, with a final 10 min extension at 72 °C. The number of cycles, the annealing temperatures, and the extension temperatures used for each gene are provided in Table 1. A few samples were highly degraded, and we could not obtain amplicons using the standard DNA extraction and PCR amplification methods. These samples were processed using a modified DNA extraction and PCR amplification protocol, following Zhao et al. (2020b). All PCR products were confirmed via electrophoresis in a 1% agarose gel, visualized under UV light, and purified using a BioFlux PCR Purification Kit (China). Purified PCR products were cycle sequenced using BigDye® Terminator v.3.1 Cycle Sequencing Kits at an annealing temperature of 50 °C for all markers. The purified Big-Dye PCR products were sequenced using an ABI 3500 Genetic Analyzer. A total of 571 new sequences were generated for this study (Supplementary Table S1).

2.2. Sequence alignment and partitioning

Sequences were aligned using MUSCLE v.3.2 (Edgar, 2004), after which they were manually checked in MEGA v.7 (Kumar et al., 2016). The program DAMBE v.6 (Xia, 2017) was used to read the sequence frame to determine the codon positions. We used MAFFT v.5 (Katoh et al., 2005) to align the *16S* sequences for a better arrangement of indels. We then used Gblocks v.0.91b (Talavera and Castresana, 2007) to eliminate poorly aligned positions and divergent regions. All protein-coding genes (*COI*, *Cyt-b*, *PRLR* and *Rag-1*) were then partitioned by codon position. We used PartitionFinder v.2.0 (Lanfear et al., 2017) under Python v.2.7 (Van Rossum and Drake, 1995) to determine the best partition scheme. Because some parameters could not be evaluated through PartitionFinder, we used jModeltest v.2 (Darriba et al., 2012) to determine those parameter settings for each partition's optimal substitution model, based on the lowest Akaike's Information Criterion (AIC) score (Supplementary Table S3). All sequences were subsequently assembled using SequenceMatrix (Vaidya et al., 2011).

We prepared three sets of alignments for different analyses: (1) the combined dataset including both mtDNA and nDNA loci (including all ingroup taxa and the two *Trachylepis* species as outgroups; this was used for the non-time calibrated analysis), (2) the combined dataset including both mtDNA and nDNA loci (including one specimen per taxon for the ingroup and all outgroup taxa; this was used for the calibration dating analysis), and (3) mtDNA (including all the ingroup taxa and only the two *Trachylepis* species as outgroup, as well as the mtDNA sequences of the *A. meleagris* species complex from Daniels et al. (2005) (*16S* GenBank accession numbers: AY683682–AY683735, *COI*: AY683736–AY683789, and *Cyt-b*: AY683790–AY683828) and Engelbrecht et al. (2013) (*16S*: JQ692450–JQ692571, *COI*: JQ692328–JQ692383, JQ692385–JQ692449), and the *A. lineatus* species complex (*A. lineatus*, *A. grayi*, *A. litoralis*, and *A tristis*) from Janse van Vuuren (2009) (*16S*: GQ259670–GQ259734, GQ292543, and *Cyt-b*: GQ259604–GQ259669, GQ292544). The mtDNA dataset was constructed to strengthen the power for investigating mtDNA structure in the *A. meleagris* and *A. lineatus* species complexes (the assembled mtDNA alignments are provided in Supplementary files S7–S10). However, we did not include these sequences in our combined dataset because only a mtDNA loci was available for these individuals.

2.3. Phylogenetic analyses

For both the mtDNA and combined datasets, we performed two independent phylogenetic analyses using Maximum likelihood (ML) and Bayesian Inference (BI). For the BI analyses on the mtDNA dataset, we removed all identical sequences before analysis to generate an ultrametric tree for further species delimitation analysis.

The ML analyses were performed using RAxML-VI-HPC (Stamatakis, 2014) implemented in CIPRES Science Gateway (Miller et al., 2010). Rate heterogeneity was allowed across partitions and the substitution model GTR-GAMMA was used, as a previous study showed that the latter model may outperform the selected GTR-CAI model (Simmons and Kessenich, 2019). We performed 1000 non-parametric bootstrap replicates to estimate the robustness of support at each node. The Bayesian Inference (BI) analyses were performed using BEAST v.2.5 (Bouckaert et al., 2019). Trees from different partitions were linked, and a Yule model selected. Site models were unlinked, a relaxed log-normal clock was used for all partitions, and clock models were linked. For the combined dataset, we used the Markov Chain Monte Carlo (MCMC) setting using 110 million generations, sampling every 10 000 generations and discarding the first 10% of samples as burn-in. The mtDNA analysis was run for 700 million generations, sampling every 10 000 generations and discarding the first 10% of samples as burn-in. Tracer v.1.6 (Rambaut et al., 2016) was used to check for convergence by determining whether the effective sample size (ESS) reached the threshold value of 200. In all analyses, a maximum clade credibility tree with a common ancestor height was annotated from the tree files of each BEAST run using TreeAnnotator v.2.5. The consensus trees were visualized with FigTree v.1.4 (Rambaut, 2012) or TreeG*raph v.2 (Stöver and Müller, 2010). We considered nodes with bootstrap support (BP) $\geq$ 70% for ML analyses (Hillis and Bull, 1993), and with posterior probability (PP) $\geq$ 0.95 for BI analyses (Huelsenbeck and Rannala, 2004) as well supported.

We did not perform independent phylogenetic analyses on our nDNA markers, since there are a limited number of mutations and parsimony informative sites on both nDNA loci. Our preliminary runs revealed poor resolution of the phylogenetic relationships among taxa when using only the nuclear data, with overall low support values at each branch. As an alternative, we examined genetic relationships between all currently recognized species and hidden candidate species (suggested by our species delimitation analysis) using a haplotype network analysis. We constructed a TCS network in the program PopART v.1.7 (Clement et al., 2002) using statistical parsimony analysis on the two nDNA markers independently.

2.4. Species delimitation

We used four different species delimitation approaches to infer species boundaries. Firstly, we used the *p*-distance approach with MEGA v.7 to calculate the uncorrected *p*-distances for only the *16S* and *Cyt-b* genes, since these two genes had better sampling coverage (based on the proportion of parsimony informative sites). They are also widely used for species delimitation in Acontinae (Busschau et al., 2017, Conradie et al., 2018, Pietersen et al., 2018, Zhao et al., 2019). To better visualize the pairwise distances among individuals, we created heatmaps with trees using the R packages 'tidyverse' (Wickham, 2017), 'ape' (Paradis et al., 2004) and 'gplots' (Warnes et al., 2013) implemented in R v.3.5.1 (R Core Team, 2018). We used the combined BEAST (standard analysis) tree as the background tree for plotting.

We also utilized the Bayesian implementation of the GMYC model (bGMYC) from the R package 'bGMYC' (Reid and Carstens, 2012) to delimit species. This approach allows the analysis to be applied to multiple tree samples from the posterior distribution of ultrametric trees and takes account of uncertainty across multiple tree topologies of posterior distribution. The bGMYC method allows the determination of putative taxa by generating a pairwise probability heat map among tree tips to directly visualize the probability that two nested tree tips are members of the same candidate species. We used LogCombiner (part of the BEAST package) to resample 500 trees from the posterior distribution of our BEAST run on the mtDNA dataset and used these resampled trees as input trees for the analysis. The outgroups in the trees file were discarded using RASP v.4.0 (Yu et al., 2020) before analysis to gain better delineation results. We ran the multiple MCMC trees with 100,000 generations, discarding the first 50,000 generations as burn-in, using a thinning interval of 200 from the input trees file. We simultaneously plotted a probabilities heatmap for visualizing the nested tips, a log posterior sampling plot, a coalescent ratio plot, and a sampling frequency plot to confirm that sampling was sufficient and even. To determine the reliability of the bGMYC run, we used the distribution of ratios of the Coalescence to Yule rates to trace the run. If the log-ratios are < 0, the speciation rate is higher than the coalescence rate, the model may not be a good fit for the data (Reid and Carstens, 2012), and the results should be interpreted with caution. As the final step, we used the R package 'P2C2M.GMYC' (Fonseca et al., 2021) to determine whether the bGMYC model fitted our dataset.

We employed the Multi-rate Poisson Tree Processing (mPTP) model to perform delimitation analyses using the mPTP server (https://www.h-its.org/software/mptp-web-server/; Kapli et al., 2017). The mPTP method incorporates intraspecific genetic diversity and runs faster. We used the mPTP model with a p-value of 0.001 as the threshold during analysis.

To address topology discordance and ILS across multiple loci (all mtDNA and nDNA loci) in species delimitation using the multispecies coalescent (MSC) model, and to evaluate the robustness of support for each candidate species (the minimal clusters), we used the STACEY package (Jones, 2017) for species delimitation and species tree estimation. The STACEY package requires defining the species tree tips that represent minimal clusters of the individuals *a priori*. Since these minimal clusters can be merged but never split to form potential species, we defined the minimal clusters as each individual sequence and let the program automatically determine the number of candidate species clusters. During the STACEY analysis, we first removed all identical sequences (based on the concatenated matrix including all loci), resulting in five reduced alignments (partitioned by gene): *16S*, *COI*, *Cyt-b*, *PRLR*, and *RAG-1*. We unlinked site models and trees between the mtDNA and nDNA loci, and all mtDNA loci were linked and treated as a single evolutionary unit. We applied an independent relaxed log-normal clock for all loci (unlinked, clock rate = 1.0). We treated all individuals as candidate species in the Taxon set, which is equal to assigning an unspecified species prior. The STACEY coalescent ploidy was set at 2.0 for the two nDNA loci, and 0.5 for the mtDNA. We implemented a Yule prior to estimate the species tree with prior settings: collapse height = 0.0001, relative death rate = 0 (without estimate), collapse weight: beta prior (1.1), bdcGrowthRate = log-normal ($M = 5$, $S = 2$); popPriorScale = log-normal ($M = -7$, $S = 2$); relativeDeathRate = Uniform (-0.5, 0.5). We used five independent MCMC runs of 200 million generations each, saving results every 20 000 generations in each analysis, and discarding the first 10% of trees as burn-in. The output file was analyzed with Tracer v.1.6 (Rambaut et al., 2016) to check for convergence. The Tracer plot indicated that convergence was reached (ESS > 200 for all parameters). We used the program SpeciesDelimitationAnalyser (Jones et al., 2015) to process the STACEY output files and examine the optimal clustering scheme of

species assignments. We discarded the first 1000 posterior trees from the STACEY output, with the other parameter settings being: collapse height = 0.001, and simcutoff = 1.0. The SpeciesDelimitationAnalyser output file was used as the input file to plot a similarity matrix in R v.3.5.1.

2.5. Species tree inference

2.5.1. Species tree inference without considering gene flow among taxa

To validate the species tree using the MSC model and to determine candidate species retrieved from our species delimitation analyses, we first used the StarBEAST2 package (Ogilvie et al., 2017) to examine whether the species tree matched the gene tree computed with our phylogenetic analysis. Like STACEY, StarBEAST2 also allows inferring species trees under the MSC assumption from multiple loci data. It considers gene tree conflicts among loci and ILS, but without considering the effect of horizontal gene transfer, gene flow, hybridization, or lineage introgression among taxa. We therefore first used StarBEAST to infer species trees under the assumption of zero gene flow and exchange across taxa.

In setting parameters and priors, we used the same partition settings as were used for the STACEY analysis in determining the site model, clock model, tree, and ploidy for the StarBEAST analysis. For the taxon sets, we used the summarized candidate species scheme (31 taxa) from our species delimitation analysis (see Discussion for details). We used a population mean of 10.0 with a pop function of "Linear with constant root" for the species tree population size of MSC. We used a relaxed log-normal prior for the clock model. We used a log-normal prior for birthRate.t:Species: M = 4.0, S = 1.25, and for popMean: M = -5.0, S = 1.2. We employed an exponential prior for clock mean (ucldMean): Mean = 1.0 in all gene loci, and a log-normal prior for clock mean standard deviation: M = 0.0, S = 1.0. We left the other prior settings as default. For the MCMC and the rest of the analytical processes, we used the same settings as with our STACEY analysis, except that we used 4 × 330 million runs for the analysis.

2.5.2. Species tree inference considering gene flow among taxa

By using all the functions of the StarBEAST package (MSC, topology conflict, ILS, and multi-locus), we also wanted to test whether gene flow, hybridization and lineage introgression could potentially have influenced the cladogenic pattern of the Acontinae, and whether the species tree differs when considering the influence of gene flow. To answer this question, we used the DENIM package (Jones, 2019) implemented in BEAST v.2.5, which has the full function of StarBEAST2 and takes account of gene flow among species or populations.

To perform the DENIM analysis, we used the same partition scheme, taxon sets, site and clock models and ploidy settings as used in the StarBEAST analysis, except that the Pop prior scale was set at 0.005. The Relatedness factor was set to 0.5, and the Migration decay scale = 0.01 for the Coalescence + Migration setting. For the species tree priors, Relative death rate was set to 0.5 (estimated) and Collapse weight was set to 0 (not estimated). Collapse weight tree prior settings were as follows: Beta (1, 1) with an offset = -0.5. We used the same manual initial tree setting as we did in the StarBEAST analysis to initialize the run. We used the same settings for the MCMC, tree annotation, and the rest of the analytic processes as we did for our StarBEAST analysis.

2.6. Divergence time dating

For the dating analysis, identical sequences were pruned to ensure that the time tree is ultrametric. Before performing divergence dating analyses, we used PAUP* v.4.0 (Swofford, 2002) to test the validity of the molecular clock assumptions using likelihood ratio tests on both the concatenated mtDNA dataset and the combined dataset. We used the combined RaxML ML tree as input tree to perform the analysis. We included only one representative sequence of each candidate species (based on our summarized candidate species from the species delimitation analysis) for the dating analysis.

For the fossil calibration dating, we used the Standard template to analyze the combined data in BEAST. In all cases, our likelihood ratio test indicated that the likelihood score with the molecular clock was far worse than the likelihood score without the molecular clock ($p < 0.0001$). Trees from different partitions were linked, clock models (clock rate = 1.0) and site models were unlinked. We used a relaxed log-normal clock for all the partitions since the molecular clock assumption was rejected in both molecular clock tests. We used the Fossilized Birth Death (FBD) model as tree prior, with an exponential prior (mean = 1.0), a beta sampling proportion FBD prior (Beta: Alpha = 2.0, Beta = 2.0), an exponential prior for the mean ucld clock rate (mean = 10.0) and the standard deviation of the ucld clock rate (mean = 0.3337).

Under the FBD model, the estimated age of the root is required to be specified with a reasonable range. The age of the root in our dating dataset corresponds to the split between the Xantusiidae and Scincidae (Zheng and Wiens, 2016). We calibrated the lower boundary as 70.6 Ma and upper boundary as 209.5 Ma (this gave a mean age of 140.05 Ma as prior value for the origin), as previously used in Pereira and Schrago (2017). The lower boundary was set according to the oldest scincid from the Late Cretaceous of North America (Rowe et al., 1992, Mulcahy et al., 2012, Pereira and Schrago, 2017); whilst the upper boundary was set according to the maximum age difference between the Xantusiidae and Scincidae (Benton et al., 2015). We constrained three nodes as the Most Recent Common Ancestor (MRCA), using the "fossil calibration" prior. We used fossil information from the literature to estimate the lower boundary of each node enforced as a monophyletic group. The upper boundary fossil information for these groups is unavailable, so we used the upper boundaries of the divergence results from Zheng and Wiens (2016) to estimate the age of the upper boundary. Our calibration constraints were: Scincinae2 (69.85 > age > 13.6 Ma), the lower boundary age of 13.6 Ma was calibrated based on fossils from the mid Miocene in North America (Holman, 1966, Voorhies et al., 1987, Joeckel, 1988, Pereira and Schrago, 2017), the upper boundary was set according to the estimated origin of Scincinae2 by Zheng and Wiens (2016); Lygosominae2 (25.97 > age > 5 Ma), the lower boundary was set according to the minimum age of an extinct fossil *Egernia* sp. (*Liopholis* for now) from the Miocene of Hungary (Maddin et al., 2013, Pereira and Schrago, 2017), while the upper boundary was set according to the estimated node age of Lygosominae2 (Zheng and Wiens, 2016); and Lygosominae1 (72 > age > 13.6 Ma), the lower boundary was calibrated according to the fossil *Tropidophorus bavaricus* (Böttcher et al., 2009, Böhme, 2010, Pereira and Schrago, 2017), the upper boundary was set according to the estimated origin of Lygosominae1 (Zheng and Wiens, 2016). We used these three groups as calibration constraints because both fossil information and DNA sequences (which match the markers used in this study) are available for these groups (Supplementary Table S2). We fixed the net diversification rate as lambda – mu = 0.04 lineage/million years (Feldman et al., 2016, Heinicke et al., 2017). For the MCMC settings, each analysis comprised four independent runs of 110 million generations, giving 440 million generations in total, with sampling every 5000 generations and the first 10% of sampled trees discarded as burn-in.

Thereafter, the trees and log files of the four independent runs were checked with Tracer v.1.6 (Rambaut et al., 2016) for convergence, to determine whether the ESS reached the threshold value of 200.

3. Results

3.1. Phylogeny and phylogeography

Our combined phylogeny (Fig. 2 and Supplementary Figure S1) showed four major monophyletic clades (Clades A–D) for *Acontias* and one monophyletic clade (Clade E) for *Typhlosaurus*, which were retrieved by all analytical approaches. The BI and ML analyses revealed that members of the genus *Acontias* were distinct from *Typhlosaurus*. Nevertheless, some relationships among the five major clades were poorly resolved in all methods. The combined phylogeny (Fig. 2) revealed overall low support (BP < 70 or PP < 0.95) or no support at nodes between Clade C and Clades A and B, and between Clades A and B when using the ML method.

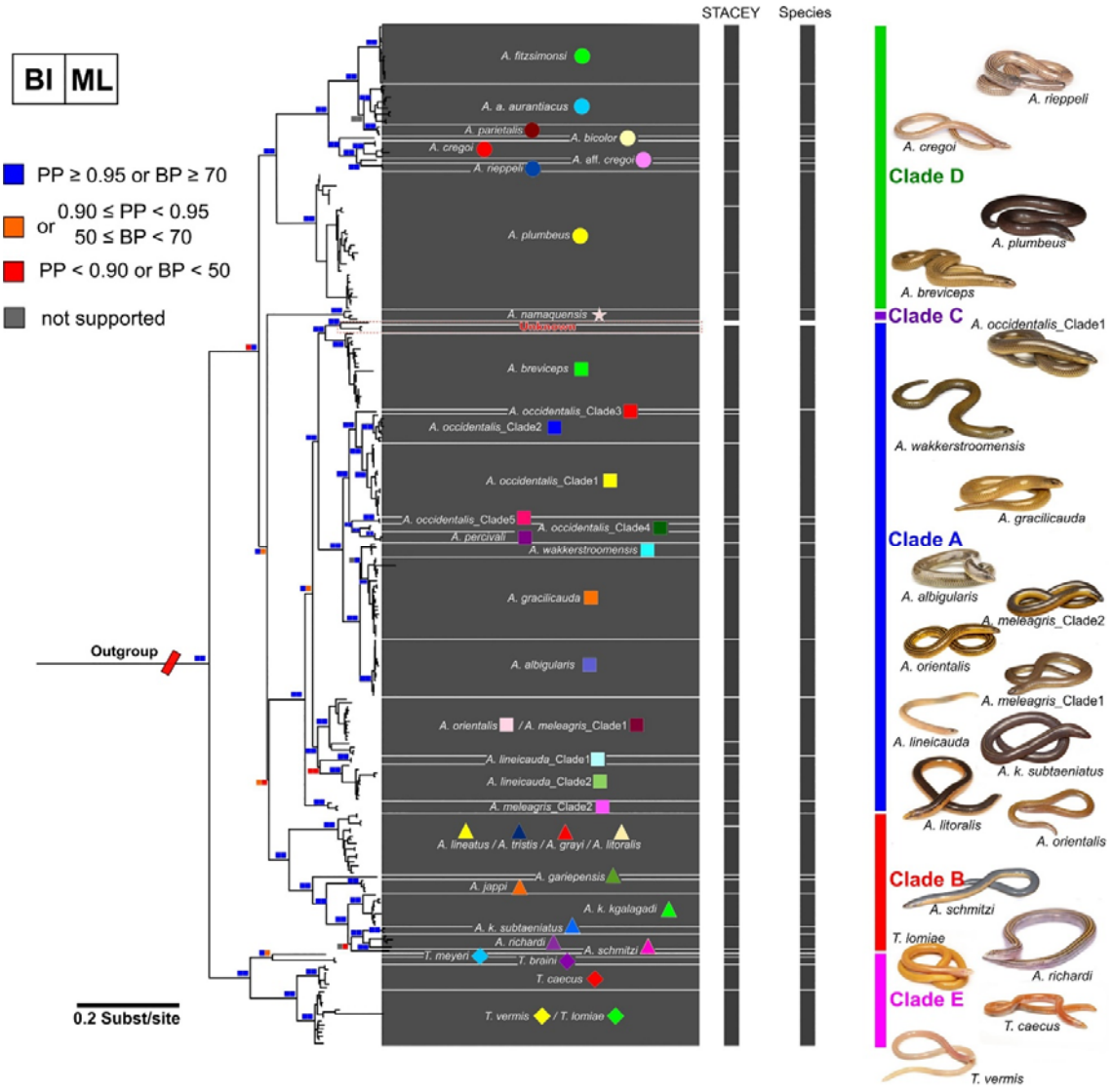

Fig. 2. Tree topology derived from the best scoring phylogram of the Maximum Likelihood (ML) analysis with the combined dataset. The support values for the two phylogenetic reconstruction approaches, Bayesian Inference (BI) and ML, are given at each node. The putative species assignment and clade information is provided for each sample. The barplots on the right represent the minimal clustering scheme suggested by the STACEY analysis, and the proposed species scheme from this study, respectively. Colours and symbols represent species from the different clades.

Clade A is generally widespread (Fig. 3A–B), its range broadly spreading into the Kalahari Basin, the southern coast, and interior plateau west of the eastern GE. Two main lineages were found in Clade A, the *A. meleagris* species complex (which occurs along the southern coast of South Africa) forming one lineage and the rest of the species forming the other (Fig. 3A–B). The two *A. meleagris* lineages occur in the CFR. Of the five lineages present in the MPA, only *A. breviceps* and the two *A. lineicauda* lineages are exclusive to it. The *A. meleagris* lineage of Clade A is only present in the WRZ and ARZ, whilst the rest of the species in Clade A only occur in the SRZ. *Acontias meleagris* Clade 2 only occurs in the WRZ. *Acontias occidentalis* did not form a monophyletic group, since *A. percivali* was placed within the *A. occidentalis* species complex (nested with *A. occidentalis* Clade 4), and these two sister species clustered with *A. occidentalis* Clade 5 and formed a branch of the *A. occidentalis* species complex. This relationship between *A. percivali* and *A. occidentalis* was supported by all phylogenetic analyses. Our *PRLR* network revealed clear divergence among the five *A. occidentalis* clades (Fig. 4). One *A. occidentalis* specimen (*A. occidentalis*, Postmasburg7) unexpectedly clustered with two *A. breviceps* samples (PenhoekPass5 and PenhoekPass8; Supplementary Figure S1). This clustering scheme was robustly supported by both combined and mtDNA results (BP $\geq$ 70 or PP $\geq$ 0.95). However, none of our nDNA TCS networks supported this relationship since all nDNA results revealed no diagnosable difference between this unusual specimen and other samples of *A. occidentalis* Clade 1 from the same locality (Fig. 4).

Surprisingly, both combined (Fig. 2) and mtDNA (Fig. 5 and Supplementary Figure S2) phylogenies and nDNA TCS networks (Fig. 4) indicated that the *A. meleagris* species complex was not monophyletic, but rather, Clade 1 grouped with *A. orientalis* and this clustering scheme was generally supported by all analyses. *Acontias meleagris* Clade 2 formed a single branch as sister taxon to a group including all other species of Clade A, resulting in the paraphyly of *A. meleagris*. The two distinctive *A. lineicauda* clades (Clades 1 and 2) were supported by all our analyses except the nDNA network (as nDNA data were absent in Clade 1), although the support on monophyletic relationship between the two clades was weak (BP < 50, PP < 0.90) across all datasets and methods.

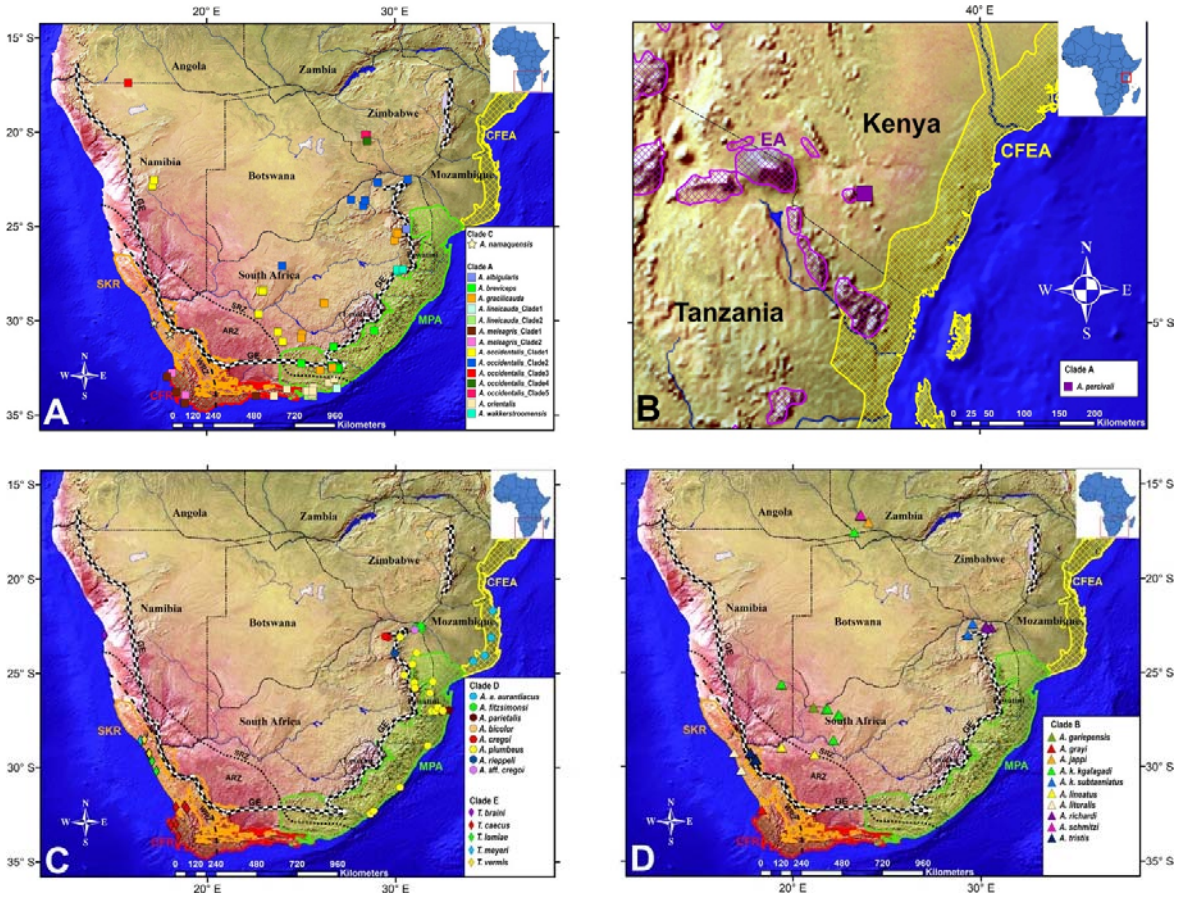

Fig. 3. Sampling sites for all *Acontias* and *Typhlosaurus* individuals used in this study. A: Clades A (excluding material from Engelbrecht et al. 2013) and C, B: *Acontias percivali*, C: Clades D and E, D: Clade B (excluding material from Janse van Vuuren 2009). The colour scheme used to represent species in the map is the same as that of the phylogenetic trees. The global biodiversity hotspots are highlighted: Cape Floristic Region (CFR, red), Succulent Karoo Region (SKR, orange), Maputaland-Pondoland-Albany (MPA, green), Coastal Forests of East Africa (CFEA, yellow), and Eastern Afromontane (EA, purple). Some biogeographically relevant features are indicated, including the Great Escarpment (GE), major rivers (in blue), and the rainfall zones (winter rainfall zone = WRZ, summer rainfall zone = SRZ, and aseasonal rainfall zone = ARZ).

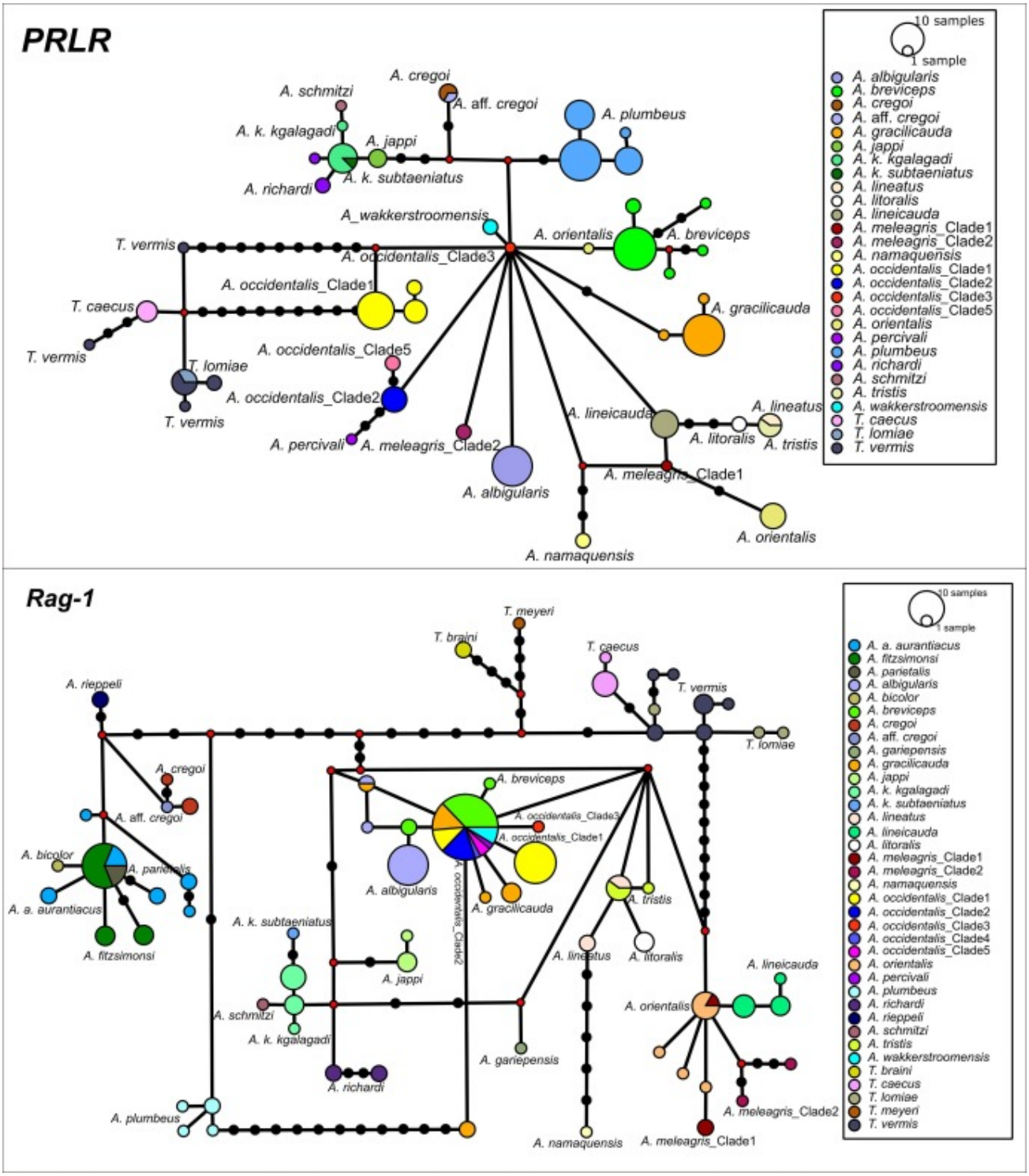

Fig. 4. TCS haplotype network based on two nDNA markers: *PRLR* and *Rag-1*. Each black dot represents a mutation step, whilst the small red dot represents the vertex.

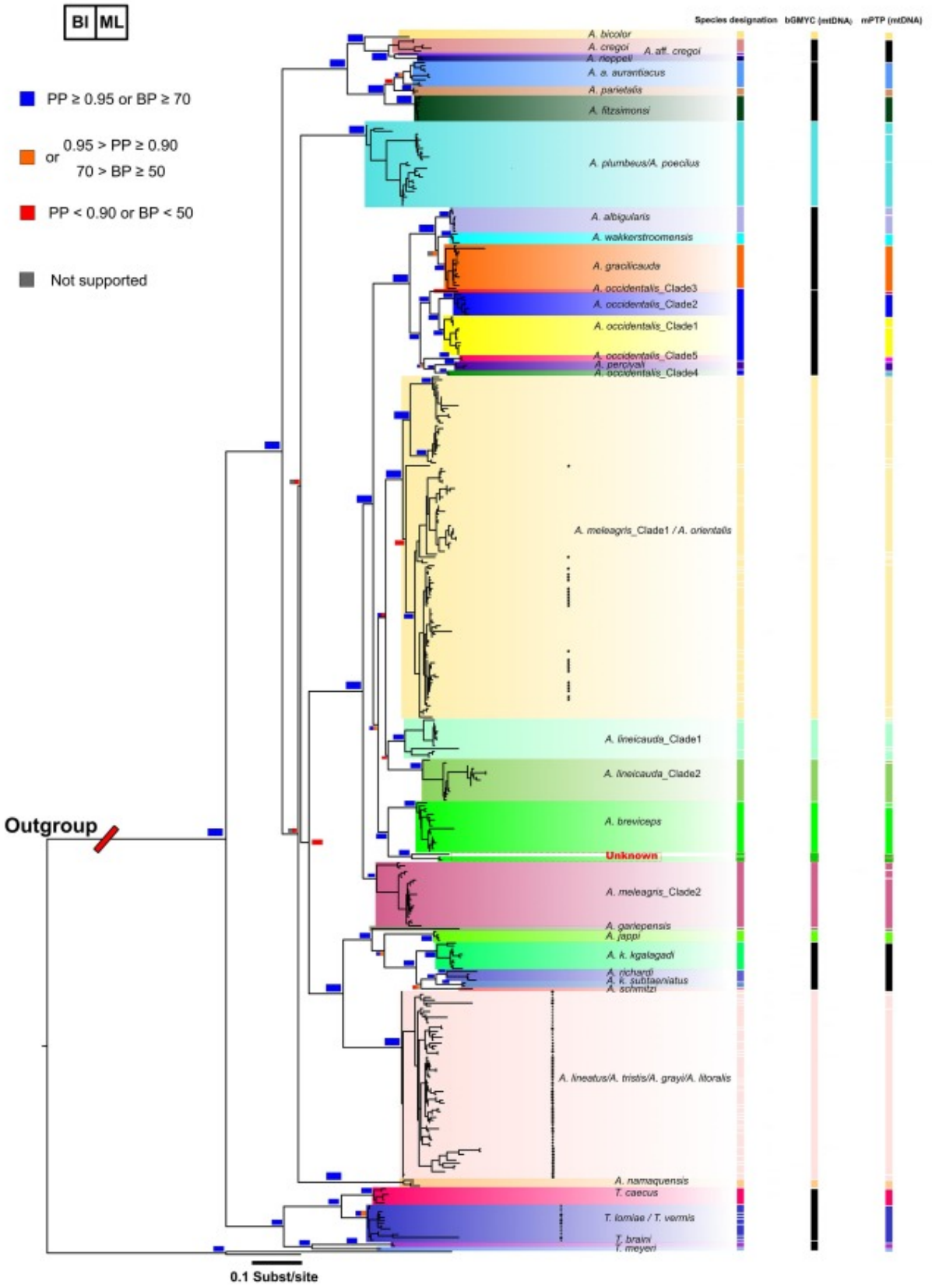
BI ML
PP ≥ 0.95 or BP ≥ 70
or 0.95 > PP ≥ 0.90 70 > BP ≥ 50
PP < 0.90 or BP < 50
Not supported
Species designation
bGMYC (mtDNA)
mPTP (mtDNA)
A. bicolor
A. cregoi
A. aff. cregoi
A. reppeli
A. a. aurantiacus
A. parietalis
A. fitzsimonsi
A. plumbeus/A. poecilus
A. albigularis
A. wakkerstroomensis
A. gracilicauda
A. occidentalis_Clade3
A. occidentalis_Clade2
A. occidentalis_Clade1
A. occidentalis_Clade5
A. percival
A. occidentalis_Clade4
A. meleagris_Clade1 / A. orientalis
A. lineicauda_Clade1
A. lineicauda_Clade2
A. breviceps
Unknown
A. meleagris_Clade2
A. garlepensis
A. jappi
A. k. kgalagadi
A. richardi
A. k. subtaeniatus
A. schmitzi
A. lineatus/A. tristis/A. grayi/A. litoralis
A. namaquensis
T. caecus
T. lamiae / T. vermis
T. braini
T. meyeri
Outgroup
0.1 Subst/site

Fig. 5. Best scoring ML tree topology retrieved with the mtDNA dataset (including data from Engelbrecht et al., 2013, Janse van Vuuren, 2009). Barplots on the right represent the different species delimitation results based on the mtDNA dataset. Black blocks indicate that the species was not supported by that specific method, or two or more groups were not significantly different from each other. The white punctuation without an outline represents putative species boundaries. Stars represent material assigned to *A. orientalis*, triangles indicate material assigned to *A. tristis*, circlesrepresent material assigned to *A. lineatus*, squares show material assigned to *A. grayi*, and diamonds indicate material assigned to *A. litoralis*.

Clade B consists of two major lineages: the first consists of the West Coast group present in the SKR, which occurs on both sides of the western GE, and only found in the WRZ and ARZ. The second lineage occurs on the outskirts of the Kalahari Basin or east of the GE (Fig. 3D). *Acontias richardi* is the sister to *A. k. subtaeniatus*, and this relationship was supported in all the analyses. All our results support the clustering of *A. schmitzi*, (*A. k. subtaeniatus* + *A. richardi*), and *A. k. kgalagadi*, but the placement of *A. schmitzi* within the group was uncertain, since the support values were low for all analyses (BP < 50, PP < 0.90). None of our analyses revealed a sister relationship between *A. k. subtaeniatus* and *A. k. kgalagadi*. The placement of *A. gariepensis* and *A. jappi* was generally stable and supported by all datasets. The four West Coast *Acontias* species (*A. lineatus*, *A. grayi*, *A. litoralis* and *A. tristis*) were not differentiated from each other but were fused into a single group, and this was supported by all our analyses.

Clade C is restricted to the SKR and western coastal side of the western GE (Fig. 3A). The monotypic Clade C contains only *A. namaquensis*, whose phylogenetic position remains unclear, since the different analytical methods generated different topographic placements and node support was weak (BP < 50, PP < 0.90).

Clade D occurs exclusively on the coastal side of the eastern GE or on the eastern GE itself. *Acontias parietalis* and *A. plumbeus* occur in the MPA hotspot, and *A. a. aurantiacus* nested within the CFEA hotspot exclusively. Clade D is dominated by closed habitat species (Fig. 3C). Clade D consists of two subclades, namely a subclade comprising *A. plumbeus* with a sister group consisting of *A. bicolor*, *A. cregoi*, *A. rieppeli*, *A. parietalis*, *A. a. aurantiacus* and *A. fitzsimonsi*. This topology was strongly supported by both our combined analysis and our nDNA network. A sample of *A. cregoi* (PEM R25080) was unexpectedly lumped with *A. rieppeli*, resulting in a new putative taxon, *A.* aff. *cregoi,* which was strongly supported by the combined and mtDNA analyses. In the nDNA networks, *A. cregoi* and *A. rieppeli* were not differentiated in either nDNA gene.

The *Typhlosaurus* group occurs in the SKR (except for *T. braini* which falls outside the SKR) and the west coast side of the GE (occurring along the west coast of South Africa and Namibia, Fig. 3C). None of our analyses were able to distinguish *T. vermis* from *T. lomiae*. A sister relationship between the species pairs (*T. braini* + *T. meyeri*)+(*T. vermis/T. lomiae* + *T. caecus*) occurring either side of the Orange River was supported by the combined and mtDNA analyses. Both the nDNA *PRLR* and *Rag-1* networks revealed incomplete separation between *T. caecus* and *T. vermis*. The separation between the northern Orange River group (*T. braini* + *T. meyeri*) and southern Orange River group (*T. vermis/T. lomiae* + *T. caecus*) was also supported by *Rag-1*.

Despite limited parsimony informative sites in both *PRLR* and *Rag-1*, the nDNA TCS network analysis generally supported our phylogeny (Fig. 4), with the majority of species and species complexes being supported by our nDNA network. The genetic distance between Clade D (mostly closed habitat, only present on the coastal side of the eastern GE) and Clades A–C

(mostly open habitat, and mostly present on the interior plateau side of the GE) were substantially different. Besides this, the majority of clades, species complexes or groups that were supported by the combined and mtDNA datasets were diagnosable by the nDNA network. Possible hybridization between *A. breviceps* (only present in the SRZ) and *A. orientalis* (only present in the WRZ) was revealed by the *PRLR* network.

3.2. Species delimitations

Overall, the single locus species delimitation results from the different methods generated ambiguous results for our species designations as indicated in the mtDNA phylogeny (Fig. 5 and Supplementary Figure S2). The mPTP method generally supported our assumed species scheme, except that it did not differentiate *A. k. kgalagadi*, *A. k. subtaeniatus*, *A. richardi* and *A. schmitzi*. Besides this, the mPTP results also exhibited some over-splitting of our assumed species, particularly in the *A. meleagris* species complex.

The bGMYC MCMC plot (not shown) indicates that convergence was reached during the run. However, the rate plot with "checkrates" function revealed that several ratios of the Coalescence to Yule rates sampled during the analysis were close to or below zero. A repeat of the bGMYC run gave similar results. This indicates that our dataset may not have fitted the bGMYC model. Under the latter model, the results were generally very conservative, lumping *A. a. aurantiacus*, *A. parietalis* and *A. fitzsimonsi* into one species; lumping *A. albigularis*, *A. wakkerstroomensis* and *A. gracilicauda* into a single species; lumping *A. k. kgalagadi*, *A. k. subtaeniatus*, *A. richardi* and *A. schmitzi* into a single species; lumping *T. caecus* and *T. vermis/T. lomiae* into a single species; and finally lumping *T. braini* and *T. meyeri* into a single species. The P2C2M.GMYC analysis results suggest that our dataset violated the GMYC model ($p = 0.03$), implying that the GMYC model may not be suitable for our dataset.

The minimal cluster retrieved from the multi-locus delimitation method STACEY generally revealed a great degree of concordance with our species assumptions (Fig. 2 and Supplementary Figure S3). Notwithstanding this, the STACEY results suggested the lumping of *A. a. aurantiacus* and *A. parietalis*, *A. cregoi* and *A. rieppeli*, *A. percivali* and *A. occidentalis* Clade 4, and *A. k. subtaeniatus* and *A. richardi*. The separation between *A. percivali* and *A. occidentalis* Clade 4, and between *A. k. subtaeniatus* and *A. richardi* are, however, still diagnosable according to the similarity matrix (Supplementary Figure S3). When ignoring the single individual *A.* aff. *cregoi*, *A. rieppeli* can be fully separated from *A. cregoi*. Furthermore, the three clades of *A. plumbeus*, two clades within *A. meleagris*/*A. orientalis*, and two clades within the West Coast *Acontias lineatus* species complex were suggested to be separate groups by the STACEY similarity matrix. The STACEY SMC-Tree showed low support (PP < 0.90) for the monophyly of the clades in the *A. occidentalis* species complex (Clades 1–3), the two *A. lineicauda* clades, and for *A. albigularis* and *A. wakkerstroomensis*. It showed moderate support (0.95 > PP ≥ 0.90) for the grouping of *A. fitzsimonsi*, *A. a. aurantiacus* and *A. parietalis,* and between the eastern and northern clades of *A. plumbeus*. The relationships among the four *Acontias* clades were generally poorly resolved, as the support value for each branch was low (PP < 0.90). However, the monophyly of all other species groups was strongly supported (PP ≥ 0.95).

Our candidate species-level uncorrected *p*-distance matrix for *16S* revealed that the greatest interspecific genetic distance was between *A. occidentalis* and *Typhlosaurus* species (Supplementary Table S4, Supplementary Figure S4). The highest *p*-distance of 11.34% was between the unknown lineage of the *A. occidentalis* species complex of Clade A and *T. meyeri*,

whilst the lowest distance of 1.38% was between *A. wakkerstroomensis* and *A. albigularis*. The highest intraspecific *p*-distance of 2.24% was within *A. lineicauda*. In the case of *Cyt-b*, the greatest interspecific distance (16.61%) was between *T. braini* and *A. parietalis*, whilst the lowest interspecific distance (3.43%) was between *A. wakkerstroomensis* and *A. gracilicauda*. The highest intraspecific *p*-distance (3.83%) was in *A. plumbeus* (Supplementary Table S5, Supplementary Figure S5).

Regarding the *p*-distances and the "barcoding gap", the histogram of the distance matrix for both *16S* (Supplementary Figure S4) and *Cyt-b* (Supplementary Figure S5) did not reveal two obvious peaks (corresponding to the intraspecific and interspecific distances, respectively), particularly for the *Cyt-b* gene. The theoretical "barcoding gap" could thus not be clearly observed in the matrices of either gene. In the matrix of both the *Cyt-b* and *16S* genes, the majority of the intraspecific blocks were distinctive and matched our proposed candidate species allocations, although to a greater extent in the former gene. The *16S* matrix failed to distinguish between *A. schmitzi* and *A. richardi*, between *A. richardi* and *A. k. subtaeniatus*, and between *A. jappi* and *A. gariepensis*. Similar conservative results were observed in *A. occidentalis* and among *A. wakkerstroomensis*, *A. albigularis*, and *A. gracilicauda*.

3.3 Species tree inference

Under the non-gene flow model inferred with StarBEAST, the MSC species tree topology (Fig. 6A) suggested a similar relationship (with a similar support value at each node) among taxa as described by our combined concatenated gene tree retrieved from the standard phylogenetic analysis (Fig. 2), with only the placements of *A. namaquensis* and *A. wakkerstroomensis* differing. However, the relationships among the four major *Acontias* clades were still not resolved (PP < 0.90 at all corresponding nodes).

The DENIM model, which accounts for the possible influence of gene flow, hybridization and introgression, clustered the unknown lineage of *A. occidentalis* (*A. occidentalis*_Postmasburg7) with *A. occidentalis* (Fig. 6B). This unknown lineage grouped with *A. breviceps* in the combined phylogeny, mtDNA, and MSC (StarBEAST) analyses. The other parts of the species tree topology and the support values were similar to those of the StarBEAST tree.

3.4 Divergence time dating

Our dating results (Fig. 7) revealed that the divergence between the genera *Acontias* and *Typhlosaurus* started about 27 Ma during the early Oligocene. The age of the node when divergence started in *Acontias* was about 21 Ma during the early Miocene, whilst for *Typhlosaurus,* divergence started about 16 Ma, also in the early to mid-Miocene. Similar to our phylogenetic reconstruction findings, the results of the fossil calibration dating using the combined dataset exhibited topological uncertainty in terms of the relationships among the four major clades of *Acontias*. The uncertainty of the topological placement was pronounced for Clades B and C. Results indicated that most of the divergence events within the subfamily Acontinae occurred during the Miocene. The age of the node signalling the beginning of diversification in Clade A was about 10 Ma, for Clade B about 15 Ma, for Clade D about 17 Ma, and for Clade E about 16 Ma.

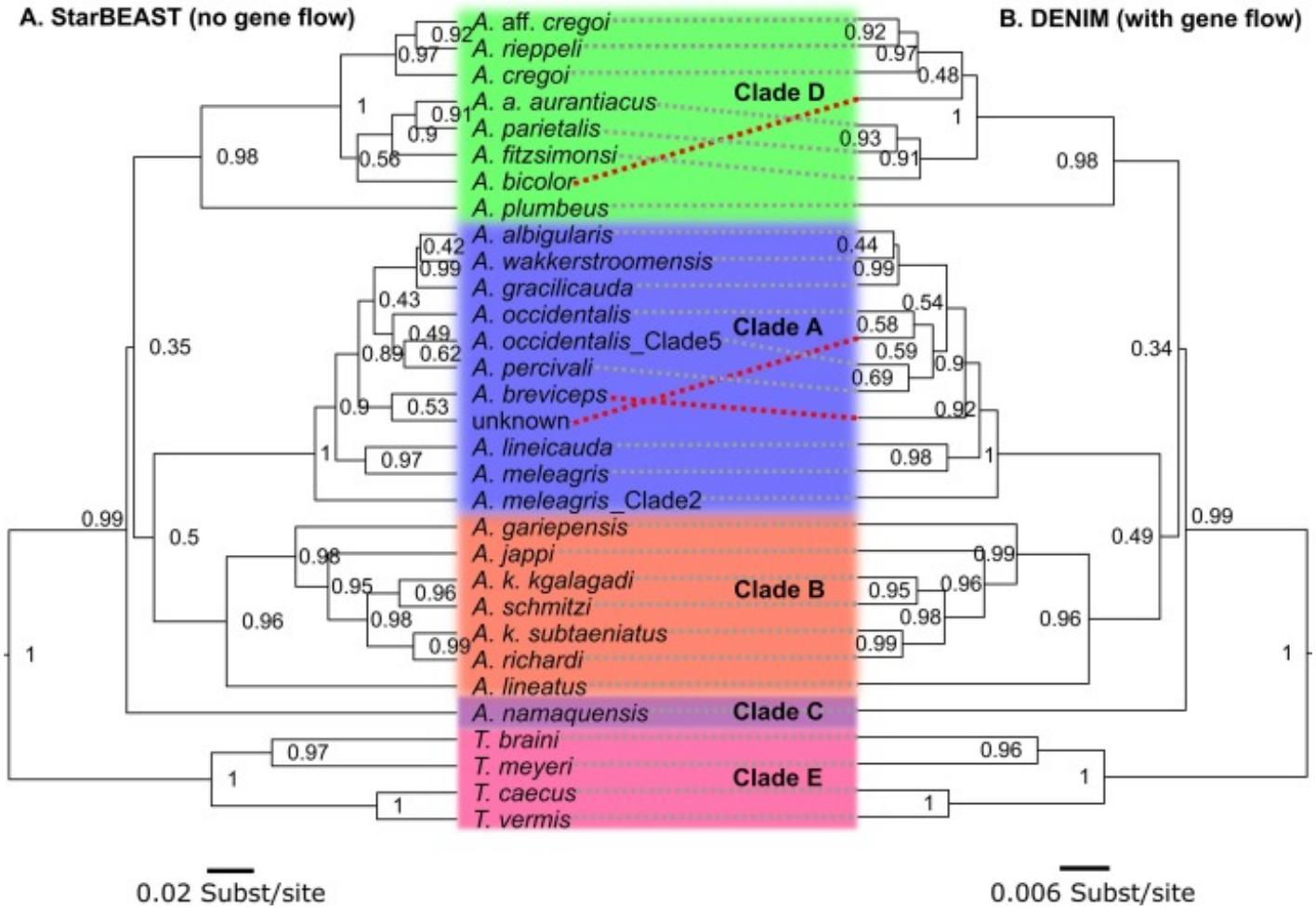

Fig. 6. Species tree comparison between A) species tree inferred with StarBEAST analysis (not considering gene flow) and B) species tree retrieved from DENIM analysis (considering gene flow). The placement of taxa revealing substantial topological conflicts are marked with red dotted lines. Nodal support values are given as posterior probabilities (PP).

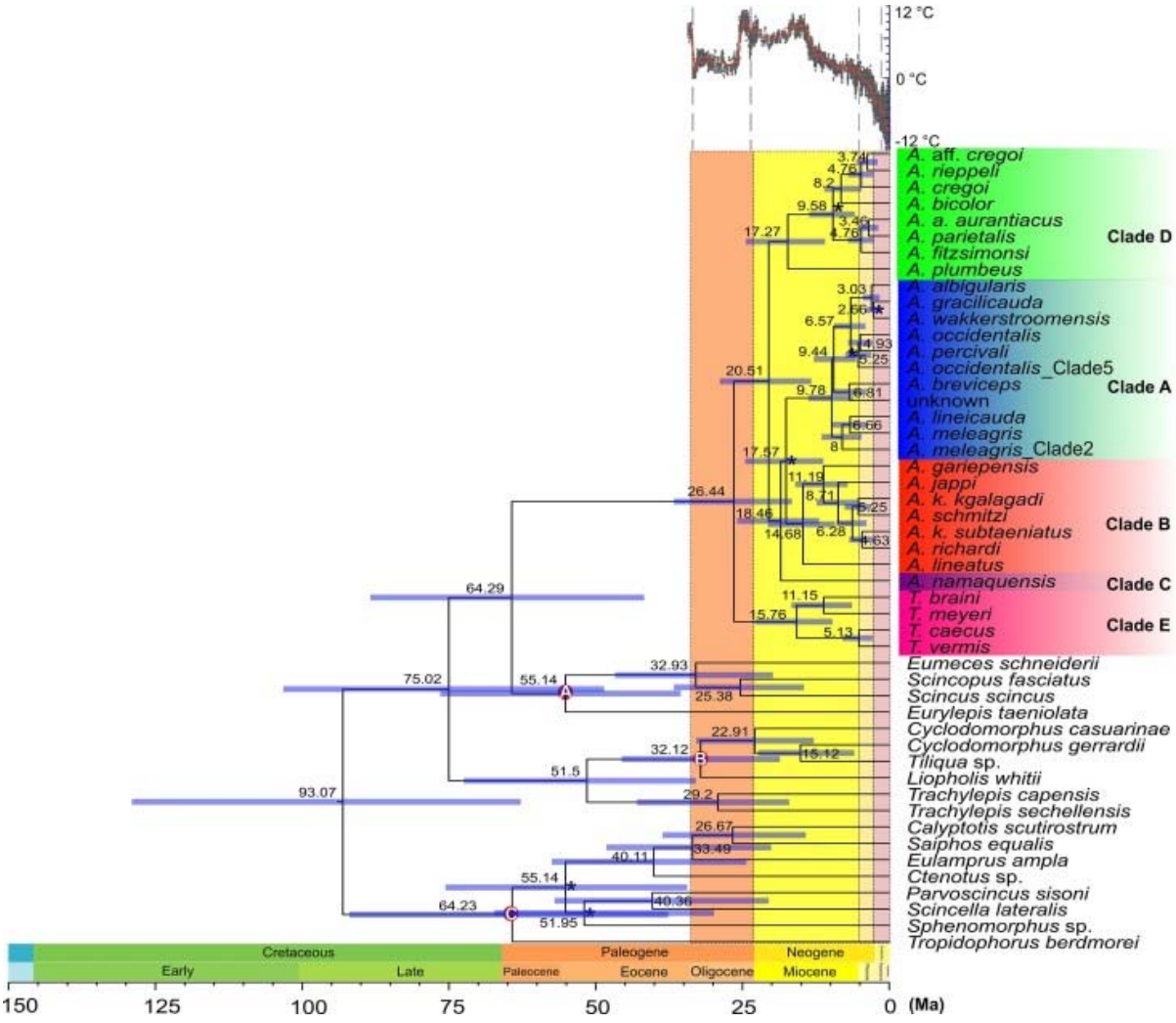

Fig. 7. Time calibrated tree using the total evidence dataset (only one specimen per taxon) retrieved from BEAST. The blue bar represents 95% height posterior density (HPD) of the estimated divergence time interval; the age of each critical divergence node is given at the tree branches. The three red dots represent the fossil calibration points, A: subfamily Scincinae2, B: subfamily Lygosominae2, and C: subfamily Lygosominae1. The background temperature fluctuation with a global scale modified from Zachos et al. (2001) is given at the top. Nodes with low support values (PP < 0.95) are marked with asterisks, whilst nodes with high support values are left blank.

4. Discussion

4.1. Phylogeny and "ghost introgression"

Our phylogenetic analyses generally supported the existence of 30 Acontinae species, with many of the assumed species also supported by our nDNA network (Fig. 4). The monophyly of *Acontias* and *Typhlosaurus* was well supported. Despite the limited informative sites, our phylogeny and nDNA networks (on both nDNA markers) revealed a great genetic distance (by mutation stage) between *Acontias* and *Typhlosaurus*, implying a substantial divergence between the two taxa. We discovered four major clades in *Acontias* (Clade A–D, Fig. 2, Fig. 3) and a single clade in *Typhlosaurus* (Clade E), each of which had robust statistical support across the different phylogenetic reconstruction approaches. However, the phylogenetic

relationships among the four clades of *Acontias* were generally poorly resolved. A further factor to consider is that the combined topology may have been more influenced by the more informative and faster-evolving mtDNA than the nDNA. Notwithstanding this, Fisher-Reid and Wiens (2011) found that combined (mtDNA and nDNA) multi-locus analyses were not dominated by the mtDNA because of its larger number of informative sites.

Compared to Daniels et al., 2006, Lamb et al., 2010, the major lineages revealed a high degree of congruence, particularly when comparing the combined trees. The five Acontinae clades retrieved by this study also matched the tree topologies generated by Lamb et al. (2010), except for minor differences. Several interesting findings in this study have not been recorded by previous studies for both *Acontias* and *Typhlosaurus*. Regarding Clade A, we discovered five clades in *A. occidentalis*, all of which were strongly supported by our phylogenetic analyses. At least three species are believed to be subsumed under *A. occidentalis* as currently construed, namely, *A. occidentalis* species one (Clade 1–3), *A. occidentalis* species two (Clade 5), and *A. percivali* (merging *A. percivali* with *A. occidentalis* Clade 4). Despite the unparalleled extreme geographic and low genetic distances between *A. percivali* and *A. occidentalis* (Clade 4), the evidence suggests that a period of extreme aridity led to the formation of a broad continuous arid corridor across central and southern Africa during the Pliocene and Pleistocene glacial cycles (Verdcourt, 1969, Van Zinderen Bakker and Mercer, 1986). The divergence between *A. percivali* and *A. occidentalis* (Clade 4) falls within the Pliocene which exhibits a good match with this event. We assume that *A. percivali* once had a broad distribution across this arid corridor and that aridification during the Pliocene could have isolated two populations (one to the north in Tanzania, one to the south in Zimbabwe) resulting in the current geographic pattern. Interestingly, a similar biogeographic pattern was also reported for two sympatric skink species (*Mochlus afer* and *M. sundevallii*) occurring in the same arid corridor (Freitas et al., 2018). Further sampling and morphological analyses are needed to verify whether *A. percivali* is conspecific with *A. occidentalis* Clade 4. Also noteworthy is the finding that the five clades revealed some diagnosable differences in the conservative nDNA network for the *PRLR* gene. Geographically, they also appear to occur in distinctive regions.

Our results revealed that *A. meleagris* is not monophyletic, with *A. meleagris* Clade 2 being only distantly related to all other *A. meleagris* clades. The non-monophyly of *A. meleagris* is supported by all phylogenetic analyses and the two conservative nDNA networks, suggesting that the taxonomy of *A. meleagris* deserves re-evaluation. We also found that *A. orientalis* was not genetically different from *A. meleagris* Clade 1. This finding is concordant with the results of Daniels et al., 2005, Engelbrecht et al., 2013. It therefore suggests the merging of *A. meleagris* Clade 1 and *A. orientalis*. Daniels et al. (2005, 2009) and Engelbrecht et al. (2013) proposed that *A. lineicauda* should merely be regarded as a morph of *A. meleagris*. However, both our study and that of Daniels et al. (2006), using a more comprehensive set of gene loci (three mtDNA and two nDNA loci), revealed that *A. lineicauda* is a monophyletic group and that its taxonomic status should remain valid. Our dating analysis also revealed a relatively deep divergence time between the two *A. lineicauda* clades (~7 Ma), indicating substantial intraspecific genetic divergence. So far, no morphological evidence supports the separation of these two clades. Furthermore, when comparing the topologies between our combined and mtDNA datasets, the segregation between the two clades became even less distinct after adding additional samples from a wider geographic range in the mtDNA phylogeny. It is therefore more realistic and reasonable to treat the two *A. lineicauda* clades as a single taxon. Overall, our results suggest three distinct lineages that could be treated as candidate species in the *A. meleagris* species complex. Our phylogeny and nDNA network confirmed the monophyly of the group comprising *A. albigularis*, *A. gracilicauda*, and *A. wakkerstroomensis*. Furthermore,

all the results confirmed that *A. albigularis* and *A. breviceps* (both previously regarded as *A. breviceps*) were distantly related. These findings corroborate the results of Busschau et al., 2017, Conradie et al., 2018.

In Clade B, the West Coast *Acontias* group (*A. grayi*, *A. litoralis*, *A. tristis* and *A. lineatus*) was returned as sister to the group comprising *A. gariepensis*, *A. k. kgalagadi*, *A. k. subtaeniatus*, *A. richardi*, *A. schmitzi* and *A. jappi*. This sister relationship was strongly supported by most of our analyses as well as by Lamb et al. (2010). None of our analyses revealed any distinct genetic differences among the four West Coast *Acontias* species. This finding corroborates the conclusion of Janse van Vuuren (2009), suggesting that the four species of the West Coast *Acontias* should be merged into a single species.

Clade C consists of a single species, *A. namaquensis*, whose topological placement remained unclear across all analyses in this study and in Lamb et al. (2010). Studies involving genome-level single-nucleotide polymorphism (SNP) markers could possibly help to solve its phylogenetic placement.

All our analyses strongly supported the relationships between *A. gariepensis*, *A. k. kgalagadi*, *A. k. subtaeniatus*, *A. richardi*, *A. schmitzi* and *A. jappi*. Most of the analyses placed *A. schmitzi* as the sister taxon to "*A. richardi* + *A. k. subtaeniatus*", but the low support values also highlight the uncertainty of this placement. We found that *A. k. kgalagadi* and *A. k. subtaeniatus* are not sister taxa. Instead, all our analyses support *A. k. subtaeniatus* as the sister taxon to *A. richardi*, and thus we suggest treating *A. k. subtaeniatus* as a full species.

Within Clade D, *A. plumbeus* was sister to the group consisting of "*A. bicolor* + *A. cregoi* + *A. rieppeli* + *A. parietalis* + *A. a. aurantiacus* + *A. fitzsimonsi*", as supported by most of our analyses. Within the *A. aurantiacus* species complex, despite a robustly supported monophyly, none of our analyses yielded strong support for the divergence between *A. parietalis* and *A. aurantiacus*. Furthermore, our nDNA networks did not reveal a significant difference between *A. parietalis*, *A. a. aurantiacus* and *A. fitzsimonsi*. According to Pietersen et al. (2018), the divergence between *A. a. aurantiacus* and *A. fitzsimonsi* was relatively shallow. However, the three species are likely separated by large rivers which they appear unable to cross and also show consistent morphological differences, suggesting reproductive isolation despite the low genetic divergences (Pietersen et al., 2018). Furthermore, the three species occur in very different habitats. The range of *A. a. aurantiacus* is completely covered by the CFEA, a habitat dominated by coastal forest. *Acontias parietalis* only occurs in the MPA, a habitat covered by woodland or forest, while *A. fitzsimonsi* occurs in savanna and is restricted to north-eastern South Africa (Branch, 1998, Marchese, 2015, Noss et al., 2015). These profound ecological differences are likely to have fostered allopatric divergence (Fitzpatrick et al., 2009). Further studies dealing with hybridization and reproductive isolation among these three assumed species are necessary. In another branch of Clade D (which includes *A. bicolor*, *A. cregoi* and *A. rieppeli*), one *A. cregoi* specimen surprisingly grouped with *A. rieppeli*. This is unlikely to be a case of either mtDNA introgression (because mtDNA was similar between the two taxa) or hybridization due to secondary contact (as the nDNA markers did not reveal a diagnosable difference between the two species). Rather, we suggest that the uniform *A. cregoi* colour morph that occurs in north-western Kruger National Park (South Africa) may represent a cryptic species, and thus tentatively refer to it as *A.* aff. *cregoi* until more work is done on this population. Although the genetics show low divergence between *A. rieppeli* and *A. cregoi*, they are morphologically distinct (Fitzsimons, 1943, Broadley and Greer, 1969, Branch, 1998, Daniels et al., 2006), including among others that *A. rieppeli* possesses a unique immovable,

semi-transparent lower eyelid versus no externally visible eye in *A. cregoi* (Fitzsimons, 1943, Broadley, 1968). Furthermore, as the ranges of these two species do not overlap and as their ecologies differ markedly (Broadley, 1968, Bates et al., 2014), hybridization is unlikely.

Our results revealed no diagnosable genetic difference between *T. lomiae* and *T. vermis*. This is despite these two species showing consistent morphological differences (Haacke, 1986). This suggests that *T. lomiae* and *T. vermis* may be merged into a single species, although a targeted study including increased genetic sampling and a concomitant morphological study are required to assess this hypothesis. A sister relationship between Namibian *T. braini* + *T. meyeri* and South African *T. lomiae/vermis* + *T. caecus* was well supported, with the two sister groups occurring in distinctly separate geographical regions. Our nDNA networks nevertheless indicated a genetic overlap between *T. vermis* and *T. caecus*, which may imply that there is still some gene flow between them and that they likely diverged quite recently. Our dating results showed that the divergence between *T. vermis* and *T. caecus* only occurred quite recently at about 5 Ma, which supports our hypothesis of potential continued gene flow.

Interestingly, one *A. occidentalis* specimen which morphologically resembled *A. occidentalis* Clade 1 and grouped in Clade 1 in the nDNA network (supported by all analyses), surprisingly grouped with a subclade of *A. breviceps* (marked as "unknown") in the mtDNA analysis and was thus assigned to *A. breviceps*. Such a huge mitochondrial-nuclear phylogenetic conflict could have arisen from hybridization or secondary contact (Benavides et al., 2007). However, the geographic distribution of *A. breviceps* does not overlap with that of *A. occidentalis* (Broadley and Greer, 1969, Bates et al., 2014, Conradie et al., 2018). Therefore, the assumption of secondary contact or hybridization would be highly unlikely. Instead, we believe that this mitochondrial-nuclear discordance is a result of "ghost introgression".

Evolution is a continuous process in which most lineages go extinct without leaving transitional forms (Ottenburghs, 2020). Some of these extinct lineages were obviously closely related and may have hybridized with those lineages that gave rise to extant species. The genetic signatures resulting from these ancient introgression events may still be found in genomes in the present-day, a phenomenon referred to as "ghost introgression" (Ottenburghs, 2020). These "ghost introgressions" may cause deep mitochondrial divergence and mitochondrial-nuclear discordance, leading to situations where the actual divergence between species or populations is indeed shallower than observed in mtDNA genomes (Spottiswoode et al., 2011, Hogner et al., 2012, Zhang et al., 2019). This deep mitochondrial-nuclear discordance phenomenon of "ghost introgression" has been found in a wide variety of organisms (Zhang et al., 2019), from birds (Spottiswoode et al., 2011, Hogner et al., 2012) to invertebrates (Kvie et al., 2013, Giska et al., 2015). A recent genome-based study, however, provided some solid evidence for the existence of these so-called "ghost introgressions" as the cause of deep mitochondrial genome divergence, and it suggested that "ghost introgressions" were widely overlooked (Zhang et al., 2019). "Ghost introgression" has also been observed in many other lizard species (Benavides et al., 2007, McGuire et al., 2007, Haenel, 2017, Barley et al., 2019, Yang et al., 2020). Moreover, a recent study discovered the possibility of horizontal mitochondrial gene transfer between frog species in the genus Pelophylax (Ivanov et al., 2019), and although no evidence for horizontal gene transfer has yet been recorded in lizards, this requires further investigation.

4.2. Species predelimitations

Pairwise divergence values can be used as an informative blueprint for species delimitation alongside other evidence to assist in taxonomic inferences (Ferguson, 2002). Uncorrected *p*-

distances in particular have been found to be positively correlated with the degree of postzygotic isolation between taxa (Malone and Fontenot, 2008). Nonetheless, it should not be regarded as an absolute indicator in defining species boundaries. In our case, the minimum interspecific *p-distance* of the Acontinae for the two most informative genes was ~ 2.2% for *16S* and ~ 3.8% for *Cyt-b*. These thresholds for delineating taxon boundaries in *Acontias* were close to the criteria suggested by several previous authors for both genes (Daniels et al., 2005, Daniels et al., 2006, Daniels et al., 2009, Busschau et al., 2017, Conradie et al., 2018, Pietersen et al., 2018). However, strictly applying these thresholds for delineating *Acontias* and *Typhlosaurus* species may result in a reduction in some of the currently recognised taxa that are well supported by other analyses. Regarding the bGMYC models, our analyses suggested that the models were unsuitable for our dataset, and the models predicted unrealistic and very conservative species delineations. This implies that caution is needed when using the bGMYC model for species delimitation and that it is crucial to perform a model test with statistical methods to ensure model fit before commencing analyses.

When comparing our results obtained from different species delimitation approaches, we found those obtained with the MSC model-based STACEY to be the most conservative, but also the most plausible in delineating species in Acontinae. Most of our species assumptions were strongly supported by STACEY, with minor deviations. We used the minimal STACEY cluster scheme as a blueprint whilst also considering other evidence (e.g., morphology, phylogeny, and ecology) to inform our proposed species scheme, and we used this proposed species scheme in our species tree inference analysis. Although the STACEY minimal cluster retrieved three candidate species in *A. plumbeus*, considering their conservative morphological appearance, morphometric measurement and nDNA structure (Zhao et al., 2019), we treated the three clades as a single species. STACEY also merged *A. a. aurantiacus* and *A. parietalis*, and our phylogeny generally also revealed low support for splitting these two taxa. Nonetheless, considering their distinctive biogeographic distribution and consistent morphological differences, we suggest that their species status be retained. The similarity matrix revealed clear differences between *A. rieppeli* and *A. cregoi*, when *A.* aff. *cregoi* was excluded. The STACEY analysis also revealed subdivisions in *A. meleagris* Clade 1, *A. lineatus* and *A. lineicauda*, but these subdivisions did not match any diagnosable morphological groups, geographic features, or previous taxonomic names and the support values for these clades on the SMC-tree were also low. We therefore propose ignoring these subdivisions and maintaining the original species designations. We lumped *A. occidentalis* Clades 1–3 as suggested by the STACEY matrix and low node support of the SMC-tree topology. STACEY merged *A. occidentalis* Clade 4 and *A. percivali* and this is supported by their similar morphological appearance and relatively close genetic relationship. Regarding *A. subtaeniatus* and *A. richardi*, despite the minimal cluster analysis suggesting that they should be treated as a single species, we propose treating them as separate taxa because of their strongly supported reciprocal monophyly, distinct morphology, and robust node support on the SMC-tree.

Overall, the phylogenetic and multi-locus MSC species delimitation analyses generally provided robust support for the validity of our species assumptions in this study. We therefore propose a total of 30 taxa (and one "unknown" lineage in the *A. occidentalis* species complex) for the Acontinae (the proposed species allocation scheme given in Fig. 2 and Table 2).

Table 2. List of currently recognized Acontinae taxa and taxa requiring further taxonomic work or standing to be synonymized (in bold).

No.	Currently recognized taxon	Proposed taxon
1	*Acontias aurantiacus aurantiacus*	*Acontias aurantiacus aurantiacus*
2	*Acontias fitzsimonsi*	*Acontias fitzsimonsi*
3	*Acontias parietalis*	*Acontias parietalis*
4	*Acontias albigularis*	*Acontias albigularis*
5	*Acontias breviceps*	*Acontias breviceps*
6	***Acontias cregoi***	***Acontias cregoi* + *Acontias* aff. *cregoi***
7	*Acontias gariepensis*	*Acontias gariepensis*
8	*Acontias gracilicauda*	*Acontias gracilicauda*
9	***Acontias grayi***	**Synonymise with *Acontias lineatus***
10	*Acontias jappi*	*Acontias jappi*
11	*Acontias kgalagadi kgalagadi*	*Acontias kgalagadi*
12	*Acontias kgalagadi subtaeniatus*	*Acontias subtaeniatus*
13	*Acontias lineatus*	*Acontias lineatus*
14	*Acontias lineicauda*	*Acontias lineicauda*
15	***Acontias litoralis***	**Synonymise with *Acontias lineatus***
16	***Acontias meleagris***	***Acontias meleagris* sp. 1 + sp. 2**
17	*Acontias namaquensis*	*Acontias namaquensis*
18	***Acontias occidentalis***	***Acontias occidentalis* sp. 1 + sp. 2**
19	***Acontias orientalis***	**Synonymise with *Acontias meleagris* sp. 1**
20	*Acontias percivali*	*Acontias percivali*
21	*Acontias plumbeus*	*Acontias plumbeus*
22	*Acontias richardi*	*Acontias richardi*
23	*Acontias rieppeli*	*Acontias rieppeli*
24	*Acontias schmitzi*	*Acontias schmitzi*
25	***Acontias tristis***	**Synonymise with *Acontias lineatus***
26	*Acontias wakkerstroomensis*	*Acontias wakkerstroomensis*
27	*Typhlosaurus braini*	*Typhlosaurus braini*
28	*Typhlosaurus caecus*	*Typhlosaurus caecus*
29	***Typhlosaurus lomiae***	**Synonymise with *Typhlosaurus vermis***
30	*Typhlosaurus meyeri*	*Typhlosaurus meyeri*
31	*Typhlosaurus vermis*	*Typhlosaurus vermis*

4.3. Species tree inference

Our species trees inferred with the two MSC models, StarBEAST (gene flow free model) and DENIM (gene flow model), revealed a high degree of concordance in terms of tree topology and node support, except that our StarBEAST species tree grouped the "unknown" *A. occidentalis* individual with *A. breviceps*, as did most of our other phylogenetic analyses. In contrast, our DENIM species tree assigned the "unknown" individual to *A. occidentalis*, which fits its morphological appearance and our nDNA phylogeny. Furthermore, the MigrationAnalyser of DENIM provided strong support for the scenario of mtDNA introgression rather than nDNA hybridisation, since a strong signal of mtDNA transfer between *A. occidentalis* and *A. breviceps* was detected. Although we noted that most of the inferred introgression events or mito-nuclear conflicts are associated with nodes that are not well supported, the DENIM species trees generated identical topologies at these nodes during testing (results not shown), which indicates that it was likely not a random event. Furthermore, our other phylogenetic analyses and the STACEY similarity matrix supported the unusual *A. occidentalis* sample as belonging to the *A. occidentalis* group, rather than *A. breviceps*. The

morphology of this specimen also indicates that it is an *A. occidentalis* and not *A. breviceps*. More importantly, the distribution of the entire *A. occidentalis* group does not overlap with that of *A. breviceps* (Bates et al., 2014). Therefore, we believe it is reasonable to assume that the unique genetic pattern of the "unknown" *A. occidentalis* individual was a result of a mtDNA introgression event with *A. breviceps*, rather than hybridization or secondary contact. Regarding the situation of *A. rieppeli* and *A. cregoi*, our DENIM results failed to detect any gene flow signal between these two species, and the DENIM species tree suggested that *A.* aff. *cregoi* is sister to *A. rieppeli* rather than *A. cregoi*. Furthermore, out *Rag-1* network revealed clear divergence between *A. rieppeli* and (*A. cregoi* + *A.* aff. *cregoi*), but there is no diagnosable divergence between *A. cregoi* and *A.* aff. *cregoi*. This implies that *A.* aff. *cregoi* was not the result of cross-over or introgression between *A. rieppeli* and *A. cregoi*. Morphologically, the uniform blacked colour in *A.* aff. *cregoi* differentiate it from *A. cregoi* with stripped colour pattern. Thus *A.* aff. *cregoi* is more likely to be an independent lineage, but further study is required to verify this. In addition, we also detected a strong signal of gene flow among *A. albigularis*, *A. gracilicauda*, and *A. wakkerstroomensis* with *RAG-1*, and between *T. caecus* and *T. vermis* with *PRLR*. These findings reveal possible gene flow or hybridization in these groups.

Our species tree topology generally corroborated the phylogenetic relationships retrieved by our other phylogenetic analyses. Nonetheless, the node supports at certain parts of the species tree were relatively weak compared to our gene tree phylogeny. This happened in the *A. aurantiacus* species complex, *A. occidentalis* species complex, and between *A. albigularis* and *A. wakkerstroomensis*, and is possibly a consequence of gene flow or hybridization. Besides this, different gene loci (particularly the nDNA loci) retain different functions and evolutionary information, so that the branching patterns among different genes also differ (Lemmon and Lemmon, 2012, Liu et al., 2018). Incongruence among gene tree topologies of different loci, ILS, and gene flow between lineages can therefore impact the species tree topology (Degnan and Rosenberg, 2006, Rosenberg, 2013). The weaker node support of the species tree (compared to the concatenated gene tree phylogeny) could also have resulted from ILS and conflicting gene tree topologies.

4.4. Diversification and biogeography of the Acontinae

The estimated divergence time between the two outgroup species, *Trachylepis capensis* and *Trachylepis sechellensis*, was ~ 29 Ma, which is very close to the ~ 30 Ma estimation of Weinell et al. (2019). Nonetheless, given that the phylogenetic relationships among Clades A–C were unsolved, interpretations based on the observed divergence times between them should be treated with caution. Three scenarios could possibly explain their current divergence: (1) allopatric divergence caused by geographic barriers, (2) allopatric divergence resulting from ecological barriers, and (3) an integrated scenario with coeffects from both the ecological and geographic barriers.

The divergence time between *Acontias* and *Typhlosaurus* dates to the late–Oligocene, approximately 27 Ma. At that time, the opening of the Drake Passage caused the cold Benguela Current to flow northwards along western South Africa (Feakins and deMenocal, 2010), resulting in the southern parts of Africa becoming progressively more arid (Burke and Gunnell, 2008). At the same time, the Antarctic ice sheet caused global cooling since the early Oligocene, and during this period the glaciers reached their maximum extent, and the icehouse conditions were widespread globally (Zachos et al., 2001). This cooling and gradual aridification possibly contributed to the diversification and separation of the ancestral

Acontinae species into distinct geographical regions, subsequently causing the respective formation of the ancestral *Acontias* and *Typhlosaurus* groups. A glaciation event commenced from the early Miocene (~23 Ma) until ~ 20 Ma, following a warm period in the late Oligocene (Zachos et al., 2001). In theory, a period characterised by warmer temperatures (late Oligocene) may have facilitated the wide dispersal of the ancestral *Acontias* group across southern Africa. Thereafter, the glacial cooling event could have restricted their range, facilitating isolation and speciation. According to Böhme (2003), the mid-Miocene Climate Optimum (MMCO) 17–15 Ma resulted in a temperature rise, followed by a substantial decline in temperature from 14 Ma onwards (Zachos et al., 2001). Our dating results suggest that the diversification of Clade B started ~ 15 Ma, which falls into the MMCO interval. These episodic processes of warming and cooling possibly resulted in the wide distribution of the ancestral lineage of Clade B on the west coast and the interior plateau at the start of the warm MMCO period. The mid-Miocene cooling 14 Ma would have initiated the divergence between the west coast group and other Clade B members. Most of the divergence events in both *Acontias* and *Typhlosaurus* occurred in the mid- (e.g., Clade B, Clade D and *Typhlosaurus*) to late-Miocene (majority of cladogenic events in all clades), with a few events in the early Pliocene, which support our hypothesis. The climatic shifts of the mid- to late-Miocene cooling (Zachos et al., 2001) have been shown to shape diversification patterns and caused major cladogenic events in many other lizard genera in southern Africa (Tolley et al., 2008, Stanley and Bates, 2014: Medina et al., 2016, Heinicke et al., 2017, Weinell and Bauer, 2018, Busschau et al., 2019). Similar well-supported evidence was also found in fossorial reptile species (Portillo et al., 2018, Portillo et al., 2019, Busschau et al., 2020). Our dating results corroborate these findings and imply that major diversification events in *Acontias* and *Typhlosaurus* were possibly also driven by the Miocene cooling. Furthermore, the rain shadow effect resulting from the warm Agulhas Current and uplift of the eastern GE contributed to climate variation on both sides of the GE in the late Miocene, resulting in aridification of the interior plateau while maintaining a moist subtropical climate along the east coast (Neumann and Bamford, 2015, Sepulchre et al., 2006). This likely drove speciation for Clades A and D. It would therefore seem that ecological barriers in the form of climatic oscillations played a major role in shaping the bifurcation between *Typhlosaurus* and *Acontias*.

Other herpetofauna also show a similar divergence pattern. Portillo et al. (2018) suggested that the diversification of the African burrowing snakes, the aparallactines, started around 29 Ma, which concurs with our dating results for the Acontinae. The cladogenic radiation of "Clade C" of the Mabuyinae skinks (mostly occurring in southern Africa) was initiated around a similar time (~30 Ma; Weinell et al., 2019). The estimated time for the basal divergence of African vipers (genus Bitis) was ~ 26 Ma (Barlow et al., 2019). A nearly identical divergence time was also observed in the rain frogs (genus *Breviceps*), with the divergence time between the *mossambicus* and *gibbosus* groups dating back to around 28 Ma (Nielsen et al., 2018). The divergence between the leopard tortoise (*Stigmochelys pardalis*) and the tent tortoises (genus *Psammobates*) dates back to ~ 27 Ma (Kehlmaier et al., 2019). The biogeographic patterns suggest that the gradual aridification during the Oligocene likely influenced the diversification and biogeographic patterns of the herpetofauna in southern Africa.

Recent episodic climatic oscillations (e.g., periodic climatic cycles during the Pliocene and Pleistocene; Fedorov et al., 2006) and long-distance dispersal from a more recent time could have disrupted some diverging patterns for taxa at the earlier stages of diversification (Vanden Broeck et al., 2014, Helmstetter et al., 2019). Geographically, *Typhlosaurus* occurs exclusively in coastal sandy areas along the west coast of southern Africa, whilst *Acontias* are found throughout the subcontinent (Branch, 1998). Cooling and aridification in the late Oligocene

could have caused range contractions resulting in the ancestral *Typhlosaurus* lineage being restricted to the west coast, adapting to those conditions and subsequently branching off from the *Acontias* lineage. *Acontias* is currently also present along the west coast, possibly as a consequence of episodic range expansions and contractions due to the recent climatic oscillations and geomorphic changes. Recent dispersal events during the warm phase (e.g., Kalahari sand expansion; Partridge and Maud, 1987) could have facilitated the dispersal of some *Acontias* groups towards the southwestern coastal areas. Alternatively, the effects of wet and dry phase oscillations on seasonal rivers of the Kalahari drainage system and Orange River Basin could also have led to their recent dispersal through river flows or floods (Nash and Endfield, 2002, Kistin and Ashton, 2008). Although the GE established a significant geographic barrier between the west coast and the interior plateau (Clark et al., 2011), there are two west coast corridors linking these areas (Fig. 1) which would have facilitated dispersal and gene flow. Interestingly, one corridor occurs in the overlapping zone between *Acontias* (*A. namaquensis*, *A. tristis*, *A. litoralis*, and *A. lineatus*) and *Typhlosaurus* (*T. vermis*; Fig. 1, Fig. 3A, 3C and 3D), whilst the second corridor coincides with the overlap between *T. caecus* (Fig. 3C) and *A. grayi* (Fig. 3D) in the southern part of the SKR. Therefore, these recent processes could also have influenced the current complex biogeographic patterns of these species The current distribution range and insignificant genetic divergence among *Acontias* species of the west coast group suggests recent dispersal or gene flow between the west coast and interior plateau sides of the GE.

Typhlosaurus is restricted to the WRZ, but the WRZ was not the driver of its split from *Acontias* (as discussed above). Clade D is only present in the SRZ along the east coast of South Africa. It is unclear when exactly the SRZ became firmly established, but evidence suggests that the shifting of the main moisture source from the Atlantic to the Indian Ocean during the onset of major aridification around 8 Ma could have established the stable SRZ (Dupont et al., 2013). However, our estimated divergence time between Clade D and the other three clades (Clades A–C; ~21 Ma) does not match this event, which may imply that the establishment of the SRZ was not the driver for this divergence. Nevertheless, the establishment of the SRZ could possibly have influenced the later divergence within Clade A or B, as both these clades show a clearer separation in their ranges along the ARZ/SRZ boundary. The establishment of the SRZ coincides with the divergence time between *A. meleagris* Clades 1 and 2 and *A. lineicauda,* and the rest of the species of Clade A at ~ 10 Ma. This divergence time is close to the time of establishment of the SRZ ~ 8 Ma (Dupont et al., 2013). Furthermore, Hoffmann et al. (2015) suggested that the development of perennial to weakly seasonal arid conditions on the west coast was initiated in the mid-Miocene (~17–13 Ma), and that the strongly seasonal rainfall regime only began in the late Miocene ~ 8 Ma. Concordance between these times implies that the establishment of a firm seasonal rainfall pattern may have influenced the diversification in Clade A. In Clade B, the estimated divergence time between the west coast species and the rest of Clade B is ~ 15 Ma, which coincides with the time of development of weakly seasonal arid conditions on the west coast. Therefore, it seems that the establishment of seasonal rainfall influenced the diversification in both clades. Rain frogs (*Breviceps*) exhibit a similar biogeographic pattern demarcated by the ARZ/SRZ boundary (Nielsen et al., 2018). The estimated divergence time between species either side of the ARZ/SRZ line in the *Breviceps gibbosus* group was around 16 Ma which falls into the proposed period of development of perennial to weakly seasonal arid condition along the west coast (Hoffmann et al. 2015) and is very close to our estimated basal divergence of Clade B ~ 15 Ma which showed a similar biogeographic pattern.

The WRZ was established since the late Miocene (Coetzee, 1978, Siesser, 1980, Deacon, 1983, Partridge, 1997, Rommerskirchen et al., 2011). *Acontias meleagris* Clade 2 is only present in the WRZ, with the divergence time between *A. meleagris* Clade 2 and (*A. meleagris* Clade 1 + *A. lineicauda*) dating back to 8 Ma in the late Miocene. The precise concordance in time suggests that the segregation between the two *A. meleagris* clades was possibly influenced by the development of the WRZ. Interestingly, the divergence pattern of the rain frogs once again revealed strong concordance with *Acontias*, with the bifurcation times between non-WRZ species *B. acutirostris* + *B. fuscus* and WRZ species *B. gibbosus* + *B. rosei* + *B.montanus* dating back ~ 10 Ma to the late Miocene. Furthermore, despite the conservative nature of nDNA markers, both our nDNA genes suggested substantial segregation between the two *A. meleagris* clades. Therefore, the development of early rainfall patterns seems to have played a role in its speciation.

Subtropical woodland conditions persisted until the early Miocene (22–19 Ma; Currano, et al., 2020, Aduse-Poku et al., 2022), which matches our estimated divergence time of ~ 21 Ma between the closed forest lineage (Clade D) and the open grass habitat lineages (Clades A–C). This suggests that the shifting from closed C3 forests to open C4 grassland may have influenced the biogeographic pattern of *Acontias*. Our conservative nDNA markers also revealed profound divergence between the open and closed habitat lineages. Thereafter, C3 forests or woody plants were gradually replaced by C4 grasses from the mid to late-Miocene onwards (Cerling et al., 1997, Dupont et al., 2013), which matches further divergence within Clade D. A similar divergence time of ~ 18 Ma and biogeographic pattern was also found in rain frog lineages from closed habitats (Nielsen et al. 2018); and in the African vipers, the closed habitat lineage (*Macrocerastes*) and open habitat lineage (*Calechidna*) diverged in the early Miocene ~ 19 Ma (Barlow et al., 2019). The increase in open habitat likely caused the forest habitat to fragment and constrict, limiting closed refugia and retracting the distribution area (Cerling et al., 1997; Barlow, 2013 and 2019; Dupont et al., 2013). The continuous increase in open habitat would have triggered further cladogenic events in the late Miocene and Pliocene in the closed forest lineage of Clade D. A similar divergence pattern was also observed in the African vipers (Barlow et al., 2019), dwarf chameleons (*Bradypodion*; Tolley et al., 2008), and rain frogs (Nielsen et al., 2018).

The observed patterns of diversification could have also resulted from the formation of the GE and continental erosion associated with the uplift between the late Oligocene and early Miocene (Partridge and Maud, 1987, Burke and Gunnell, 2008, Moore et al., 2009, Feakins and deMenocal, 2010), as our estimated divergence time between *Typhlosaurus* and *Acontias* coincides with this uplift event. Besides this, the epeirogenic uplifts of the Oligocene–Miocene and Pliocene–Pleistocene periods established many modern mountain ranges and the resultant Kalahari Depression (Dingle et al., 1983, Birkenhauer, 1991). If it is assumed that the GE was a profound vicariance barrier which resulted in the allopatric divergence between *Typhlosaurus* and *Acontias,* the presence of *A. namaquensis*, the west coast *Acontias* species group, and the *A. meleagris* species complex on the coastal side of the GE must be the result of dispersal at a later stage, particularly for the west coast *Acontias* species group, given the insignificant genetic divergence among species in this group. The three corridors on the southern side of the GE (Fig. 1) would facilitate the dispersal of ancestral lineage of the *A. meleagris* species complex during the early Miocene warm interval.

Within *Acontias*, an unusual phylogeographic pattern was observed, in that the genus split into two branches: one branch consisting only of Clade D (which only occurs to the east of the eastern GE), while the second branch consists of Clades A–C and generally occurs inland of

the eastern GE. Previous authors suggested that the uplift of southern Africa first occurred in the early Miocene ~ 23 Ma (Partridge, 1998, Partridge and Maud, 1987, Partridge and Maud, 2000). By contrast, Burke, 1996, Burke and Gunnell, 2008 propose that uplift commenced ~ 30 Ma and that it has been developing continuously. Other evidence also suggests that southern Africa experienced further massive uplifting during the past 20 million years, particularly in the eastern part of the GE (McCarthy and Rubidge, 2005; Norman & Whitfield, 2006; McCarthy, 2013). Clade D diverged from other *Acontias* clades about 17 Ma, with the divergence time coinciding with the massive uplifting event (McCarthy and Rubidge, 2005; Norman & Whitfield, 2006; McCarthy, 2013). In Clade D (except *A. plumbeus*), our dating results suggest that diversification began ~ 10 Ma in the late Miocene, and that the majority of further cladogenic events occurred ~ 8–4 Ma. These dating results match the late-Miocene tectonic uplift in eastern Africa ~ 8 Ma, which led to a drastic reorganisation of atmospheric circulation and gave rise to strong aridification and paleoenvironmental changes in south-eastern Africa (Sepulchre et al., 2006). The tectonic uplift in eastern Africa also substantially influenced the cladogenic diversification patterns in other fossorial species, such as burrowing snakes (Portillo et al., 2018) and thread snakes (Busschau et al., 2020). This geological evidence largely corroborates our dating results of the divergence between Clade D and Clades A–C. The aridification and paleoenvironmental shifting would have facilitated isolation of populations due to retracting refugia and may have facilitated speciation in Clade D in eastern and southern Africa. Therefore, we may reasonably deduce that the co-effects of early Miocene uplift, the cooling effect of glaciation, and the development of the warm Agulhas Current drove the divergence between the two major branches of Clade D and Clades A–C.

Neither ecological barriers nor geographic barriers can, in isolation, explain the current diversification patterns and an integrative scenario whereby both processes played a role appears to be the most plausible explanation. In summary, by comparing biogeographic patterns against temporal and spatial scales between different species of the Acontinae and other southern African herpetofauna, we suggest that the interaction between progressively increasing cooling (Zachos et al., 2001) and its consequential aridification (Burke and Gunnell, 2008, Neumann and Bamford, 2015), epeirogenic uplift (Partridge, 1997, Burke and Gunnell, 2008, Moore et al., 2009), the establishment of variable rainfall patterns (Siesser, 1980, Deacon, 1983, Partridge, 1997, Rommerskirchen et al., 2011, Dupont et al., 2013, Hoffmann et al., 2015), and the gradual expansion of open habitats (Cerling et al., 1997, Dupont et al., 2013, Neumann and Bamford, 2015) were likely the major driving forces in shaping the diversification and biogeographic patterns of the Acontinae. Nonetheless, other factors like the episodic waxing and waning between erosion and uplift (Partridge, 1997, Burke and Gunnell, 2008, Moore et al., 2009), between open and closed habitat (Dupont et al., 2013, Portillo et al., 2018, Barlow et al., 2019), in glacier fluctuation (Zachos et al., 2001), the recent episodic climatic oscillations in the Pliocene and Pleistocene (Fedorov et al., 2006), and long-distance dispersal in more recent times (Vanden Broeck et al., 2014, Helmstetter et al., 2019) could have homogenized some of the earlier established patterns of diversification (Vanden Broeck et al., 2014, Helmstetter et al., 2019), resulting in the current complex biogeographic patterns of these organisms.

Lastly, regarding the Global Biodiversity Hotspots and their well-established conservation value on a global scale (Mittermeier et al., 2011, Williams et al., 2011, Marchese, 2015, Noss et al., 2015), the four hotspots in southern Africa harbor some critically important biodiversity refugia and potential future diversification drivers that could play crucial roles in biodiversity conservation (Clark et al., 2011). As an example, the GE serves as an important refugium for biodiversity and a potential driver for shaping allopatric diversification for a broad range of

herpetofauna (Clark et al., 2011, Nielsen et al., 2018, Barlow et al., 2019, Zhao et al., 2020a). The GE is nearly entirely covered by the SKR and MPA in South Africa. The MPA and CFEA have both undergone shrinking of closed forest habitats since the late Miocene (Dupont et al., 2013). Our study suggests that at least six taxa from four Acontinae clades occur in the SKR (at least four taxa are endemic), four taxa from two clades are present in the CFR (two endemic taxa and two potential candidate species), and six taxa from two clades occur in the MPA (two endemic taxa), with one taxon from the CFEA. The SKR, CFR, and MPA also demarcate biogeographic patterns across other herpetofauna, particularly the southern African chameleons (Tolley et al., 2008), rain frogs (Nielsen et al., 2018), African vipers (Barlow et al., 2019), and tent tortoises (Zhao et al., 2020a). Therefore, the four hotspots not only maintain high species richness and endemism for many fauna and flora species, but also serve as important reservoirs for multiple potential speciation drivers, thus retaining future diversification potential and making them critically valuable for future biodiversity conservation in southern Africa.

4.5. Future study

We recommend further study at the genomic scale (such as using genome-wide single nucleotide polymorphisms [SNPs] or double digest restriction-site associated DNA [ddRAD] markers) to not only improve the accuracy of the species tree inference, but also to clarify the relationship among the four *Acontias* clades, particularly the placement of *A. namaquensis* which has not been resolved by the present study. Genome-wide SNP markers would also facilitate the diagnosing of hybridization. Interspecific gene flow (hybridization or introgression) was shown to severely impact species tree estimations under the MSC model (Jones, 2019), and we therefore propose the use of genome-wide SNP markers to overcome this dilemma. Further ecological studies considering the link between ecological niches and diversification patterns using comprehensive statistical analyses is also recommended. Additional sampling in Botswana, Zimbabwe and Namibia (for *A. occidentalis*, *A. kgalagadi*, *A. lineatus*, *A. percivali*, and *A. gariepensis*), the filling of sampling gaps between *A. cregoi* and *A. rieppeli*, and between the two *A. lineicauda* clades are also crucial for establishing a full biogeographic paradigm for the Acontinae. Lastly, a fine-scale examination of morphological characters using both morphometric and meristic data with adequate sample sizes (at least ten specimens per taxon) will be crucial before establishing a reliable taxonomy and nomenclature for the group. Ideally, reproductive studies should also be undertaken to test how extensive hybridization is and to determine species boundaries within *Acontias* and *Typhlosaurus*, respectively.

5. Conclusion

This study used a comprehensive sampling strategy with adequate sampling covering each species complex and taxon currently recognised in the subfamily Acontinae. Our phylogeny and species delimitation analyses resolved the majority of evolutionary relationships among taxa, and also allowed investigation of the genetic structures within each species complex or specific group, and clarification of species boundaries. We analysed the phylogenetic relationships among the Acontinae species by using multiple DNA markers and found overall support for four clades in *Acontias* and a single clade in *Typhlosaurus*. However, the relationships among the four *Acontias* clades were poorly resolved, and a further genome-level study may be required to provide greater clarity. Through the well-established geological information and comparing the Acontinae biogeographic patterns with that of other southern African herpetofauna, our fossil evidence-based divergence dating results suggest that the

cladogenesis of the Acontinae was shaped by ancient climatic shifts and topographical changes. The divergence between *Typhlosaurus* and *Acontias* was possibly driven by progressive cooling and aridification caused by the opening of the Drake Passage and the epeirogenic uplift which established the GE in the late–Oligocene. Further cladogenesis of *Typhlosaurus* and *Acontias* was probably mainly driven by the Miocene cooling, uplift of the eastern GE, the gradual expansion of open habitat, establishment of variable rainfall patterns together with the influence of the warm Agulhas Current from the early Miocene onwards, the development of the cold Benguela Current, and their co-effects. Nonetheless, other recent events like the episodic waxing and waning between erosion and uplift, glacier fluctuations, episodic climatic oscillations in the Pliocene and Pleistocene, and long-distance dispersal could have homogenized some well-established divergence patterns of earlier diversifications, resulting in the current complex biogeographic patterns seen in the Acontinae. When comparing the biogeographic patterns of the Acontinae with that of other southern African herpetofauna, it is evident that the four biodiversity hotspots are not only important refugia harboring rich biodiversity and endemism, but also maintain future diversification potential for southern African herpetofauna.

Our phylogeny and species delimitation analyses proposed at least 30 species in the subfamily Acontinae, while revealing several candidate species in *A. occidentalis*, *A. meleagris* and *A. cregoi*. Long-standing evolutionary questions on the phylogenetic relationships within the *A. kgalagadi*, the *A. lineatus,* the *A. meleagris*, and the *A. occidentalis*, species complexes and *Typhlosaurus* have been satisfactorily resolved. We thus formally elevate *A. subtaeniatus* to full species and suggest further taxonomical work is needed before formally synonymising or describing further species in the other species complexes. This research thus constitutes an important baseline for further taxonomic investigations. Our findings indicate substantial gene flow between *A. gracilicauda* and *A. albigularis*, and between *T. vermis* and *T. caecus*, respectively, suggesting possible cross-over between them. We also discovered the phenomenon known as “ghost introgression” in the *A. occidentalis* species complex.

CRediT authorship contribution statement

Zhongning Zhao: Conceptualization, Methodology, Software, Visualization, Investigation, Data curation, Formal analysis, Funding acquisition, Project administration, Resources, Validation, Writing - original draft, Writing - review & editing. **Werner Conradie:** Conceptualization, Software, Visualization, Investigation, Funding acquisition, Data curation, Resources, Validation, Writing - review & editing. **Darren W. Pietersen:** Funding acquisition, Investigation, Resources, Validation, Writing - review & editing. **Gary Nicolau:** Software, Visualization, Review & editing, and Data curation. **Shelley Edwards:** Conceptualization, Methodology, Software, Visualization, Investigation, Funding acquisition, Data curation, Resources, Validation, Writing - review & editing. Stephanus Riekert: Software, Visualization, Investigation, Formal analysis. **Neil Heideman:** Conceptualization, Software, Visualization, Investigation, Funding acquisition, Data curation, Project administration, Resources, Supervision, Validation, Writing - review & editing.

Declaration of Competing Interest

The authors declare that they have no known competing financial interests or personal relationships that could have appeared to influence the work reported in this paper.

Acknowledgements

The Mpumalanga Tourism and Parks Agency (Permit No: MPB.5298 and MPB. 5492), Eastern Cape Department of Economic Development, Environmental Affairs and Tourism (Permit no. CRO 84/11CR, CRO 85/11CR, CRO 106/11CR, 43/17CR, and 44/CR), Limpopo Department of Economic Development, Environment and Tourism (Permit no. 001-CPM402-00001), Northern Cape Department of Environment and Nature Conservation (Permit no. FAUNA 624/2015) and the Zambia Wildlife Authority (ZAWA) are thanked for issuing collecting permits. The National Research Foundation (NRF) of South Africa and the University of the Free State are thanked for providing funds to cover the costs of this study under grants IFR2011041300046 and TTK160602167413. We also thank Dr. Joaquín Verdú Ricoy, who assisted with data assembly**.**

WC thanks Chris Brooks, organizer of the SAREP Aquatic Biodiversity Survey of the lower Cuito and Cuando River basins (April 2013), supported by and also involving members of the Angolan Ministry of Environment Institute of Biodiversity (MINAMB) and the Angola Ministry of Agriculture National Institute of Fish Research (INIP), who facilitated the export of voucher specimens for analysis; Brian Reeves and Jan Venter for organizing the biodiversity surveys of Eastern Cape Parks and Tourism Agency protected areas. Additional samples were donated by the South African National Biodiversity Institute (SANBI), Kyle Finn, Philip Jordaan, Bill Branch, Francois Theart, and Faansie Peacock. Alex Rebelo and Luke Kemp are thanked for their assistance in the field. Additional material was collected during the Foundation Biodiversity Information Program (FBIP)-funded Eastern Cape Forest Project and the Karoo BioGaps project. AJ would like to thank Shiela Broadley (Natural History Museum Zimbabwe) for donating samples and Jens Reissig for facilitating the transport thereof. ZZ thanks Prof. Paul Grobler for providing laboratory access, and Tyrone James Ping for his contribution of photographs.

References

Aduse-Poku, K., et al., 2022. Miocene climate and habitat change drove diversification in bicyclus, Africa's largest radiation of satyrine butterflies. Syst. Biol. 71 (3), 570–588.

Barley, A.J., de Oca, A.N.M., Reeder, T.W., Manríquez-Mor´an, N.L., Monroy, J.C.A., Hernández-Gallegos, O., Thomson, R.C., 2019. Complex patterns of hybridization and introgression across evolutionary timescales in Mexican whiptail lizards (*Aspidoscelis*). Mol. Phylogenet. Evol. 132, 284–295.

Barlow, A., Baker, K., Hendry, C.R., Peppin, L., Phelps, T., Tolley, K.A., Wüster, C.E., Wüster, W., 2013. Phylogeography of the widespread African puff adder (*Bitis arietans*) reveals multiple Pleistocene refugia in southern Africa. Mol. Ecol. 22 (4), 1134–1157.

Barlow, A., Wüster, W., Kelly, C.M., Branch, W.R., Phelps, T., Tolley, K.A., 2019. Ancient habitat shifts and organismal diversification are decoupled in the African viper genus *Bitis* (Serpentes: Viperidae). J. Biogeogr. 46 (6), 1234–1248.

Bates, M.F., Branch, W.R., Bauer, A.M., Burger, M., Marais, J., Alexander, G.J., de Villiers, M.S., 2014. Atlas and Red List of the Reptiles of South Africa, Lesotho and Swaziland. Suricata 1. Pretoria, South Africa: South African National Biodiversity Institute.

Benavides, E., Baum, R., McClellan, D., Sites, J.W., 2007. Molecular phylogenetics of the lizard genus *Microlophus* (Squamata: Tropiduridae): aligning and retrieving indel signal from nuclear introns. Syst. Biol. 56 (5), 776–797.

Benton, M.J., Donoghue, P.C., Asher, R.J., Friedman, M., Near, T.J., Vinther, J., 2015. Constraints on the timescale of animal evolutionary history. Palaeogeography Electron 18 (1), 1–106.

Birkenhauer, J., 1991. The Great Escarpment of southern Africa and its coastal forelands. A re-appraisal. Geographische Abhandlungen, Reihe B, Münchener.

Böhme, M., 2003. The Miocene climatic optimum: evidence from ectothermic vertebrates of Central Europe. Palaeogeogr. Palaeoclimatol. Palaeoecol. 195 (3–4), 389–401.

Böhme, M., 2010. Ectothermic vertebrates (Actinopterygii, Allocaudata, Urodela, Anura, Crocodylia, Squamata) from the Miocene of Sandelzhausen (Germany, Bavaria) and their implications for environment reconstruction and palaeoclimate. Paläontol. Z. 84 (1), 3–41.

Böttcher, R., Heizmann, E.P., Rasser, M.W., Ziegler, R., 2009. Biostratigraphy and palaeoecology of a Middle Miocene (Karpathian, MN 5) fauna from the northern margin of the North Alpine Foreland Basin (Oggenhausen 2, SW'Germany). Neues Jahrbuch für Geologie und Paläontologie-Abhandlungen 254 (1–2), 237–260.

Bouckaert, R., et al., 2019. BEAST 2.5: An advanced software platform for Bayesian evolutionary analysis. PLoS Comput. Biol. 15 (4), e1006650.

Branch, W.R., 1998. Field guide to the snakes and other reptiles of southern Africa, Revised edition. Struik Publishers, Cape Town, South Africa.

Branch, W.R., 1999. Reptile systematic studies in southern Africa: a brief history and overview. Transactions of the Royal Society of South Africa 54 (1), 137–156.

Broadley, D.G., 1968. A revision of the African genus *Typhlosaurus* Wiegmann (Sauria: Scincidae). Arnoldia Rhodesia 36 (3), 1–20.

Broadley, D.G., Greer, A.E., 1969. A revision of the genus *Acontias* Cuvier (Sauria: Scincidae). Arnoldia Rhodesia 4 (26), 1–29.

Burke, K., 1996. The African plate. S. Afr. J. Geol. 99 (4), 341–409.

Burke, K., Gunnell, Y., 2008. The African Erosion Surface: A Continental-scale Synthesis of the Geomorphology, Teutonics, and Environmental Change Over the Past 180 Million Years. Geological Society of America, Boulder.

Busschau, T., Conradie, W., Jordaan, A., Daniels, S.R., 2017. Unmasking evolutionary diversity among two closely related South African legless skink species (Acontinae: *Acontias*) using molecular data. Zoology 121, 72–82.

Busschau, T., Conradie, W., Daniels, S.R., 2019. Evidence for cryptic diversification in a rupicolous forest-dwelling gecko (Gekkonidae: *Afroedura pondolia*) from a biodiversity hotspot. Mol. Phylogenet. Evol. 139, 106549.

Busschau, T., Conradie, W., Daniels, S.R., 2020. One species hides many: Molecular and morphological evidence for cryptic speciation in a thread snake (Leptotyphlopidae: *Leptotyphlops sylvicolus* Broadley & Wallach, 1997). J. Zool. Syst. Evol. Res. 59 (1), 195–221.

Busschau, T., Jordaan, A., Conradie, W., Daniels, S.R., 2022. Pseudocongruent phylogeography reflects unique responses to environmental perturbations in a biodiversity hotspot. J. Biogeogr. 49 (3), 445–459.

Butler, B.O., Smith, L.L., Flores-Villela, O., 2023. Phylogeography and taxonomy of Coleonyx elegans Gray 1845 (Squamata: Eublepharidae) in Mesoamerica: The Isthmus of Tehuantepec as an environmental barrier. Mol. Phylogenet. Evol. 178, 107632.

Cerling, T.E., Harris, J.M., MacFadden, B.J., Leakey, M.G., Quade, J., Eisenmann, V., Ehleringer, J.R., 1997. Global vegetation change through the Miocene/Pliocene boundary. Nature 389 (6647), 153–158.

Chapple, D.G., et al., 2021. Conservation status of the world's skinks (Scincidae): Taxonomic and geographic patterns in extinction risk. Biol. Conserv. 257, 109101.

Chase, B.M., Meadows, M.E., 2007. Late Quaternary dynamics of southern Africa's winter rainfall zone. Earth Sci. Rev. 84 (3–4), 103–138.

Clark, V.R., Barker, N.P., Mucina, L., 2011. The Great Escarpment of southern Africa: a new frontier for biodiversity exploration. Biodivers. Conserv. 20 (12), 2543–2561.

Clement, M., Snell, Q., Walker, P., Posada, D., Crandall, K., 2002. TCS: Estimating genegenealogies. Parallel and Distributed Processing Symposium, International Proceedings 2, 184.

Coetzee, J.A., 1978. Climatic and biological changes in south-western Africa during the late Cainozoic. Palaeoecology of Africa 10, 13–29.

Conflitti, I.M., Shields, G.F., Murphy, R.W., Currie, D.C., 2014. The speciation continuum: population structure, gene flow, and maternal ancestry in the *Simulium arcticum* complex (Diptera: Simuliidae). Mol. Phylogenet. Evol. 78, 43–55.

Conradie, W., Busschau, T., Edwards, S., 2018. Two new species of *Acontias* (Acontinae, Scincidae) from the Mpumalanga Highveld escarpment of South Africa. Zootaxa 4429 (1), 89–106.

Cowling, R.M., Proches, Ş., Partridge, T.C., 2009. Explaining the uniqueness of the Cape flora: incorporating geomorphic evolution as a factor for explaining its diversification. Mol. Phylogenet. Evol. 51 (1), 64–74.

Cunningham, C.W., Blackstone, N.W., Buss, L.W., 1992. Evolution of king crabs from hermit crab ancestors. Nature 355 (6360), 539–542.

Currano, E.D., et al., 2020. Ecological dynamic equilibrium in an early Miocene (21.73 Ma) forest, Ethiopia. Palaeogeography, Palaeoclimatology, Palaeoecology, 539, 109425.

da Silva, J.M., Tolley, K.A., 2017. Diversification through ecological opportunity in dwarf chameleons. J. Biogeogr. 44 (4), 834–847.

Daniels, S.R., Heideman, N., Hendricks, M., Willson, B., 2002. A molecular phylogeny for the South African limbless lizard taxa of the subfamily Acontinae (Sauria: Scincidae) with special emphasis on relationships within *Acontias*. Mol. Phylogenet. Evol. 24 (2), 315–323.

Daniels, S.R., Heideman, N.J., Hendricks, M.G., Mokone, M.E., Crandall, K.A., 2005. Unraveling evolutionary lineages in the limbless fossorial skink genus *Acontias* (Sauria: Scincidae): are subspecies equivalent systematic units? Mol. Phylogenet. Evol. 34 (3), 645–654.

Daniels, S.R., Heideman, N.J., Hendricks, M.G., Crandall, K.A., 2006. Taxonomic subdivisions within the fossorial skink subfamily Acontinae (Squamata: Scincidae) reconsidered: a multilocus perspective. Zool. Scr. 35 (4), 353–362.

Daniels, S.R., Heideman, N.J., Hendricks, M.G., 2009. Examination of evolutionary relationships in the Cape fossorial skink species complex (Acontinae: *Acontias meleagris meleagris*) reveals the presence of five cryptic lineages. Zool. Scr. 38 (5), 449–463.

Darriba, D., Taboada, G.L., Doallo, R., Posada, D., 2012. jModelTest 2: more models, new heuristics and parallel computing. Nat. Methods 9 (8), 772.

de Queiroz, K., 2005. Ernst Mayr and the modern concept of species. Proc. Natl. Acad. Sci. 102 (suppl_1), 6600–6607.

de Queiroz, K., 2007. Species concepts and species delimitation. Syst. Biol. 56 (6), 879–886.

Deacon, H.J., 1983. An introduction to the fynbos region, time scales and palaeoenvironments. In: Deacon, H.J., Hendey, Q.B., Lambrechts, J.J.N. (Eds.), Fynbos palaeoecology: a preliminary synthesis. Council for Scientific and Industrial Research, Pretoria, South Africa, pp. 1–20.

Degnan, J.H., Rosenberg, N.A., 2006. Discordance of species trees with their most likely gene trees. PLoS Genet. 2 (5), e68.

deMenocal, P.B., 2004. African climate change and faunal evolution during the Pliocene-Pleistocene. Earth Planet. Sci. Lett. 220 (1–2), 3–24.

Dingle, R.V., Siesser, W.G., Newton, A.R., 1983. Mesozoic and Tertiary geology of southern Africa. Rotterdam, AA Balkema.

Dupont, L.M., Rommerskirchen, F., Mollenhauer, G., Schefuß, E., 2013. Miocene to Pliocene changes in South African hydrology and vegetation in relation to the expansion of C4 plants. Earth Planet. Sci. Lett. 375, 408–417.

Edgar, R.C., 2004. MUSCLE: multiple sequence alignment with high accuracy and high throughput. Nucleic Acids Res. 32 (5), 1792–1797.

Engelbrecht, H.M., Van Niekerk, A., Heideman, N.J., Daniels, S.R., 2013. Tracking the impact of Pliocene/Pleistocene Sea level and climatic oscillations on the cladogenesis of the Cape legless skink, *Acontias meleagris* species complex, South Africa. J. Biogeogr. 40 (3), 492–506.

Engelbrecht, H.M., Branch, W.R., Greenbaum, E., Burger, M., Conradie, W., Tolley, K.A., 2020. African Herald snakes, Crotaphopeltis, show population structure for a widespread generalist but deep genetic divergence for forest specialists. J. Zool. Syst. Evol. Res. 58 (4), 1220–1233.

Evlambiou, A.A., 2021. An evolutionary study of legless skinks' (*Acontias* Cuvier, 1817) head and vertebrae morphology (Unpublished master's thesis). Rhodes University, Makhanda.

Feakins, S.J., deMenocal, P.B., 2010. Global and African regional climate during the Cenozoic. In: Werdelin, L., Sanders, W.J. (Eds.), Cenozoic mammals of Africa. University of California Press, Berkeley, pp. 45–55.

Fedorov, A.V., et al., 2006. The Pliocene paradox (mechanisms for a permanent El Niño). Science 312 (5779), 1485–1489.

Feldman, A., Sabath, N., Pyron, R.A., Mayrose, I., Meiri, S., 2016. Body sizes and diversification rates of lizards, snakes, amphisbaenians and the tuatara. Glob. Ecol. Biogeogr. 25 (2), 187–197.

Ferguson, J.W.H., 2002. On the use of genetic divergence for identifying species. Biol. J. Linn. Soc. 75 (4), 509–516.

Fisher-Reid, M.C., Wiens, J.J., 2011. What are the consequences of combining nuclear and mitochondrial data for phylogenetic analysis? Lessons from *Plethodon* salamanders and 13 other vertebrate clades. BMC Evol. Biol. 11 (1), 300.

Fitzpatrick, B.M., Fordyce, J.A., Gavrilets, S., 2009. Pattern, process and geographic modes of speciation. J. Evol. Biol. 22 (11), 2342–2347.

Fitzsimons, V.F., 1943. The lizards of South Africa: Family 4. Scincidae. Transvaal Museum Memoirs 1 (1), 175–266.

Fonseca, E.M., Duckett, D.J., Carstens, B.C., 2021. P2C2M. GMYC: An R package for assessing the utility of the Generalized Mixed Yule Coalescent model. Methods Ecol. Evol. 12 (3), 487–493.

Freitas, E.S., Bauer, A.M., Siler, C.D., Broadley, D.G., Jackman, T.R., 2018. Phylogenetic and morphological investigation of the *Mochlus afer-sundevallii* species complex (Squamata:

Scincidae) across the arid corridor of sub-Saharan Africa. Mol. Phylogenet. Evol. 127, 280–287.

Giska, I., Sechi, P., Babik, W., 2015. Deeply divergent sympatric mitochondrial lineages of the earthworm *Lumbricus rubellus* are not reproductively isolated. BMC Evol. Biol. 15 (1), 217.

Gray, L.N., Barley, A.J., Poe, S., Thomson, R.C., Nieto-Montes de Oca, A., Wang, I.J., 2019. Phylogeography of a widespread lizard complex reflects patterns of both geographic and ecological isolation. Mol. Ecol. 28 (3), 644–657.

Haacke, W.D., 1986. Description of a new species of *Typhlosaurus* Wiegmann, 1834 (Reptilia: Scinidae) from the west coast of Southern Africa, with new records of related species. Ann. Transv. Mus. 34 (9), 227–235.

Haenel, G.J., 2017. Introgression of mt DNA in *Urosaurus* lizards: historical and ecological processes. Mol. Ecol. 26 (2), 606–623.

Heideman, N.J., Mulcahy, D.G., Sites Jr, J.W., Hendricks, M.G., Daniels, S.R., 2011. Cryptic diversity and morphological convergence in threatened species of fossorial skinks in the genus *Scelotes* (Squamata: Scincidae) from the Western Cape Coast of South Africa: Implications for species boundaries, digit reduction and conservation. Mol. Phylogenet. Evol. 61 (3), 823–833.

Heinicke, M.P., Jackman, T.R., Bauer, A.M., 2017. The measure of success: geographic isolation promotes diversification in Pachydactylus geckos. BMC Evol. Biol. 17 (1), 9.

Helmstetter, A.J., Buggs, R.J., Lucas, S.J., 2019. Repeated long-distance dispersal and convergent evolution in hazel. Sci. Rep. 9 (1), 1–12.

Hewitt, G.M., 1996. Some genetic consequences of ice ages, and their role in divergence and speciation. Biol. J. Linn. Soc. 58 (3), 247–276.

Hewitt, G.M., 1999. Post-glacial re-colonization of European biota. Biol. J. Linn. Soc. 68 (1–2), 87–112.

Hewitt, G.M., 2000. The genetic legacy of the Quaternary ice ages. Nature 405 (6789), 907–913.

Hewitt, G.M., 2004. Genetic consequences of climatic oscillations in the Quaternary. Philos. Trans. R. Soc. Lond. B Biol. Sci. 359 (1442), 183–195.

Hillis, D.M., Bull, J.J., 1993. An empirical test of bootstrapping as a method for assessing confidence in phylogenetic analysis. Syst. Biol. 42 (2), 182–192.

Hoetzel, S., Dupont, L.M., Marret, F., Jung, G., Wefer, G., 2015. Miocene-Pliocene stepwise intensification of the Benguela upwelling over the Walvis Ridge off Namibia. Climate Past Discuss. 11 (3), 1913–1943.

Hoffmann, V., Verboom, G.A., Cotterill, F.P., 2015. Dated plant phylogenies resolve Neogene climate and landscape evolution in the Cape Floristic Region. PLoS One 10 (9), e0137847.

Hogner, S., et al., 2012. Deep sympatric mitochondrial divergence without reproductive isolation in the common redstart *Phoenicurus phoenicurus*. Ecol. Evol. 2 (12), 2974–2988.

Holman, J.A., 1966. A small Miocene herpetofauna from Texas. Quarterly Journal of the Florida Academy of Sciences 29 (4), 267–275.

Huelsenbeck, J.P., Rannala, B., 2004. Frequentist properties of Bayesian posterior probabilities of phylogenetic trees under simple and complex substitution models. Syst. Biol. 53 (6), 904–913.

Ivanov, A.Y., et al., 2019. The first record of natural transfer of mitochondrial DNA from *Pelophylax* cf. *bedriagae* into *P. lessonae* (Amphibia, Anura). Nature Conservation Research. Заповедная наука 4 (2).

Jacobsen, N.H.G., 1987. A new subspecies of *Typhlosaurus lineatus* Boulenger 1887 (Reptilia: Scincidae) from Venda, southern Africa. Afr. Zool. 22 (4).

Janse van Vuuren, L.C., 2009. A taxonomic review of the genus Microacontias (*Scincidae: Acontiinae*) based on DNA and morphological data. University of the Free State). Doctoral dissertation.

Jansson, R., Dynesius, M., 2002. The fate of clades in a world of recurrent climatic change: Milankovitch oscillations and evolution. Annu. Rev. Ecol. Syst. 33 (1), 741–777.

Joeckel, R.M., 1988. A new late Miocene herpetofauna from Franklin County. Nebraska. Copeia 1988 (3), 787–789.

Jones, G.R., 2017. Algorithmic improvements to species delimitation and phylogeny estimation under the multispecies coalescent. J. Math. Biol. 74 (1–2), 447–467.

Jones, G.R., 2019. Divergence estimation in the presence of incomplete lineage sorting and migration. Syst. Biol. 68 (1), 19–31.

Jones, G.R., Aydin, Z., Oxelman, B., 2015. DISSECT: an assignment-free Bayesian discovery method for species delimitation under the multispecies coalescent. Bioinformatics 31 (7), 991–998.

Kapli, P., Lutteropp, S., Zhang, J., Kobert, K., Pavlidis, P., Stamatakis, A., Flouri, T., 2017. Multi-rate Poisson tree processes for single-locus species delimitation under maximum likelihood and Markov chain Monte Carlo. Bioinformatics 33 (11), 1630–1638.

Katoh, K., Kuma, K.I., Toh, H., Miyata, T., 2005. MAFFT version 5: improvement in accuracy of multiple sequence alignment. Nucleic Acids Res. 33 (2), 511–518.

Kehlmaier, C., et al., 2019. Ancient mitogenomics clarifies radiation of extinct Mascarene giant tortoises (*Cylindraspis* spp.). Sci. Rep. 9 (1), 1–7.

King, T.L., Switzer, J.F., Morrison, C.L., Eackles, M.S., Young, C.C., Lubinski, B.A., Cryan, P., 2006. Comprehensive genetic analyses reveal evolutionary distinction of a mouse (*Zapus hudsonius preblei)* proposed for delisting from the US Endangered Species Act. Mol. Ecol. 15 (14), 4331–4359.

Kistin, E.J., Ashton, P.J., 2008. Adapting to change in transboundary rivers: an analysis of treaty flexibility on the Orange-Senqu River Basin. Int. J. Water Resour. Dev. 24 (3), 385–400.

Kumar, S., Stecher, G., Tamura, K., 2016. MEGA7: molecular evolutionary genetics analysis version 7.0 for bigger datasets. Mol. Biol. Evol. 33 (7), 1870–1874.

Kvie, K.S., Hogner, S., Aarvik, L., Lifjeld, J.T., Johnsen, A., 2013. Deep sympatric mt DNA divergence in the autumnal moth (*Epirrita autumnata*). Ecol. Evol. 3 (1), 126–144.

Lamb, T., Biswas, S., Bauer, A.M., 2010. A phylogenetic reassessment of African fossorial skinks in the subfamily Acontinae (Squamata: Scincidae): evidence for parallelism and polyphyly. Zootaxa 2657 (1), 33–46.

Lanfear, R., Frandsen, P.B., Wright, A.M., Senfeld, T., Calcott, B., 2017. PartitionFinder 2: new methods for selecting partitioned models of evolution for molecular and morphological phylogenetic analyses. Mol. Biol. Evol. 34 (3), 772–773.

Lemmon, A.R., Lemmon, E.M., 2012. High-throughput identification of informative nuclear loci for shallow-scale phylogenetics and phylogeography. Syst. Biol. 61 (5), 745–761.

Liu, Y., et al., 2018. The first set of universal nuclear protein-coding loci markers for avian phylogenetic and population genetic studies. Sci. Rep. 8 (1), 1–12.

Maddin, H.C., Venczel, M., Gardner, J.D., Rage, J.C., 2013. Micro-computed tomography study of a three-dimensionally preserved neurocranium of *Albanerpeton* (Lissamphibia, Albanerpetontidae) from the Pliocene of Hungary. J. Vertebr. Paleontol. 33 (3), 568–587.

Malone, J.H., Fontenot, B.E., 2008. Patterns of reproductive isolation in toads. PLoS One 3 (12), e3900.

Marchese, C., 2015. Biodiversity hotspots: A shortcut for a more complicated concept. Global Ecol. Conserv. 3, 297–309.

McCarthy, T., 2013. The Okavango Delta and its place in the geomorphological evolution of southern Africa. S. Afr. J. Geol. 116 (1), 1–54.

McCarthy, T., Rubidge, B., 2005. The Story of Earth & Life - A Southern African Perspective on a 4.6-Billion-Year Journey. Struik Publisher, Cape Town.

McGuire, J.A., et al., 2007. Mitochondrial introgression and incomplete lineage sorting through space and time: phylogenetics of crotaphytid lizards. Evolution: International Journal of Organic. Evolution 61 (12), 2879–2897.

Medina, M.F., et al., 2016. Molecular phylogeny of *Panaspis* and *Afroablepharus* skinks (Squamata: Scincidae) in the savannas of sub-Saharan Africa. Mol. Phylogenet. Evol. 100, 409–423.

Miller, M.A., Pfeiffer, W., Schwartz, T., 2010. Creating the CIPRES Science Gateway for inference of large phylogenetic trees. In 2010 gateway computing environments workshop (GCE).

Mittermeier, R.A., Turner, W.R., Larsen, F.W., Brooks, T.M., Gascon, C., 2011. Global Biodiversity Conservation: The Critical Role of Hotspots. In: Zachos, F., Habel, J. (Eds.), Biodiversity Hotspots. Springer, Berlin, Heidelberg.

Moore, A., Blenkinsop, T., Cotterill, F., 2009. Southern African topography and erosion history: plumes or plate tectonics? Terra Nova 21 (4), 310–315.

Mulcahy, D.G., Noonan, B.P., Moss, T., Townsend, T.M., Reeder, T.W., Sites Jr, J.W., Wiens, J.J., 2012. Estimating divergence dates and evaluating dating methods using phylogenomic and mitochondrial data in squamate reptiles. Mol. Phylogenet. Evol. 65 (3), 974–991.

Myburgh, A.M., Daniels, S.R., 2022. Between the Cape Fold Mountains and the deep blue sea: Comparative phylogeography of selected codistributed ectotherms reveals asynchronous cladogenesis. Evol. Appl. 00, 1–21.

Nash, D.J., Endfield, G.H., 2002. Historical flows in the dry valleys of the Kalahari identified from missionary correspondence. S. Afr. J. Sci. 98 (5), 244–248.

Neumann, F.H., Bamford, M.K., 2015. Shaping of modern southern African biomes: Neogene vegetation and climate changes. Transactions of the Royal Society of South Africa 70 (3), 195–212.

Nielsen, S.V., Daniels, S.R., Conradie, W., Heinicke, M.P., Noonan, B.P., 2018. Multilocus phylogenetics in a widespread African anuran lineage (Brevicipitidae: *Breviceps*) reveals patterns of diversity reflecting geoclimatic change. J. Biogeogr. 45 (9), 2067–2079.

Noss, R.F., Platt, W.J., Sorrie, B.A., Weakley, A.S., Means, D.B., Costanza, J., Peet, R.K., 2015. How global biodiversity hotspots may go unrecognized: lessons from the North American Coastal Plain. Divers. Distrib. 21 (2), 236–244.

Ogilvie, H.A., Bouckaert, R.R., Drummond, A.J., 2017. StarBEAST2 brings faster species tree inference and accurate estimates of substitution rates. Mol. Biol. Evol. 34 (8), 2101–2114.

Ottenburghs, J., 2020. Ghost Introgression: Spooky Gene Flow in the Distant Past. Bioessays 42 (6), 2000012.

Paradis, E., Claude, J., Strimmer, K., 2004. APE: analyses of phylogenetics and evolution in R language. Bioinformatics 20 (2), 289–290.

Partridge, T.C., 1997. Evolution of landscapes. In: Cowling, R.M., Richardson, D.M., Pierce, S.M. (Eds.), Vegetation of southern Africa. Cambridge Univ. Press, Cambridge, pp. 1–20.

Partridge, T.C., 1998. Of diamonds, dinosaurs and diastrophism: 150 million years of landscape evolution in southern Africa. S. Afr. J. Geol. 101 (3), 167–184.

Partridge, T.C., Maud, R.R., 1987. Geomorphic evolution of southern Africa since the Mesozoic. S. Afr. J. Geol. 90 (2), 179–208.

Partridge, T.C., Maud, R.R., 2000. Macro-scale geomorphic evolution of southern Africa. In: Partridge, T.C., Maud, R.R. (Eds.), The Cenozoic of Southern Africa. Oxford University Press, Oxford, pp. 3–18.

Pereira, A.G., Schrago, C.G., 2017. Arrival and diversification of mabuyine skinks (Squamata: Scincidae) in the Neotropics based on a fossil-calibrated timetree. PeerJ 5, e3194.

Petit, R.J., Excoffier, L., 2009. Gene flow and species delimitation. Trends Ecol. Evol. 24 (7), 386–393.

Pietersen, D.W., Scholtz, C.H., Bastos, A.D., 2018. Multi-locus phylogeny of southern African *Acontias aurantiacus* (Peters) subspecies (Scincidae: Acontinae) confirms the presence of three genetically, geographically and morphologically discrete taxa. Zootaxa 4442 (3), 427–440.

Portik, D.M., Bauer, A.M., Jackman, T.R., 2011. Bridging the gap: western rock skinks (*Trachylepis sulcata*) have a short history in South Africa. Mol. Ecol. 20 (8), 1744–1758.

Portillo, F., Branch, W.R., Conradie, W., Rödel, M.O., Penner, J., Barej, M.F., Kusamba, C., Muninga, W.M., Aristote, M.M., Bauer, A.M., Trape, J.F., 2018. Phylogeny and biogeography of the African burrowing snake subfamily *Aparallactinae* (Squamata: Lamprophiidae). Mol. Phylogenet. Evol. 127, 288–303.

Portillo, F., Stanley, E.L., Branch, W.R., Conradie, W., Rödel, M.O., Penner, J., Barej, M.F., Kusamba, C., Muninga, W.M., Aristote, M.M., Bauer, A.M., 2019. Evolutionary history of burrowing asps (Lamprophiidae: Atractaspidinae) with emphasis on fang evolution and prey selection. PLoS One 14 (4), e0214889.

R Core Team., 2018. R: A language and environment for statistical computing. R Foundation for Statistical Computing, Vienna, Austria. R v.3.5.1. URL https://www.R–project.org/.

Rambaut, A., 2012. FigTree v1.4.3. Institute of Evolutionary Biology, University of Edinburgh, Edinburgh.

Rambaut, A., Suchard, M.A., Xie, W., Drummond, A.J., 2016. Tracer v1. 6. 2013. Retrieved from http:/beast. bio. ed. ac. uk/Tracer.

Rannala, B., Yang, Z., 2003. Bayes estimation of species divergence times and ancestral population sizes using DNA sequences from multiple loci. Genetics 164 (4), 1645–1656.

Reeves, P.A., Richards, C.M., 2011. Species delimitation under the general lineage concept: an empirical example using wild North American hops (Cannabaceae: Humulus lupulus). Syst. Biol. 60 (1), 45–59.

Reid, N.M., Carstens, B.C., 2012. Phylogenetic estimation error can decrease the accuracy of species delimitation: a Bayesian implementation of the general mixed Yule-coalescent model. BMC Evol. Biol. 12 (1), 196.

Rommerskirchen, F., Condon, T., Mollenhauer, G., Dupont, L., Schefuss, E., 2011. Miocene to Pliocene development of surface and subsurface temperatures in the Benguela Current system. Paleoceanography 26 (3).

Rosenberg, N.A., 2013. Discordance of species trees with their most likely gene trees: a unifying principle. Mol. Biol. Evol. 30 (12), 2709–2713.

Rowe, T., Cifelli, R.L., Lehman, T.M., Weil, A., 1992. The Campanian Terlingua local fauna, with a summary of other vertebrates from the Aguja Formation. Trans-Pecos Texas. Journal of Vertebrate Paleontology 12 (4), 472–493.

Sepulchre, P., Ramstein, G., Fluteau, F., Schuster, M., Tiercelin, J.J., Brunet, M., 2006. Tectonic uplift and Eastern Africa aridification. Science 313 (5792), 1419–1423.

Siesser, W.G., 1980. Late Miocene origin of the Benguela upswelling system off northern Namibia. Science 208 (4441), 283–285.

Simmons, M.P., Kessenich, J., 2019. Divergence and support among slightly suboptimal likelihood gene trees. Cladistics 36 (3), 322–340.

Spitzweg, C., Vamberger, M., Ihlow, F., Fritz, U., Hofmeyr, M.D., 2020. How many species of angulate tortoises occur in Southern Africa? (Testudines: Testudinidae: Chersina). Zool. Scr. 49 (4), 412–426.

Spottiswoode, C.N., Stryjewski, K.F., Quader, S., Colebrook-Robjent, J.F., Sorenson, M. D., 2011. Ancient host specificity within a single species of brood parasitic bird. Proc. Natl. Acad. Sci. 108 (43), 17738–17742.

Stamatakis, A., 2014. RAxML version 8: a tool for phylogenetic analysis and post-analysis of large phylogenies. Bioinformatics 30 (9), 1312–1313.

Stankowski, S., Ravinet, M., 2021. Defining the speciation continuum. Evolution 75 (6), 1256–1273.

Stanley, E.L., Bates, M.F., 2014. Here be dragons: a phylogenetic and biogeographical study of the *Smaug warreni* species complex (Squamata: Cordylidae) in southern Africa. Zool. J. Linn. Soc. 172 (4), 892–909.

Stöver, B.C., Müller, K.F., 2010. TreeGraph 2: combining and visualizing evidence from different phylogenetic analyses. BMC Bioinf. 11 (1), 7.

Sukumaran, J., Knowles, L.L., 2017. Multispecies coalescent delimits structure, not species. Proc. Natl. Acad. Sci. 114 (7), 1607–1612.

Swofford, D., 2002. Phylogenetic analysis using parsimony (PAUP) v. 4.0 b10. Sunderland, MA: Sinauer Associates.

Talavera, G., Castresana, J., 2007. Improvement of phylogenies after removing divergent and ambiguously aligned blocks from protein sequence alignments. Syst. Biol. 56 (4), 564–577.

Tolley, K.A., Chase, B.M., Forest, F., 2008. Speciation and radiations track climate transitions since the Miocene Climatic Optimum: a case study of southern African chameleons. J. Biogeogr. 35 (8), 1402–1414.

Tolley, K.A., Braae, A., Cunningham, M., 2010. Phylogeography of the Clicking Stream Frog *Strongylopus grayii* (Anura, Pyxicephalidae) reveals cryptic divergence across climatic zones in an abundant and widespread taxon. Afr. J. Herpetol. 59 (1), 17–32.

Tolley, K.A., Bowie, R.C., Measey, J.G., Price, B.W., Forest, F., 2014. The shifting landscape of genes since the Pliocene: terrestrial phylogeography in the Greater Cape Floristic Region. In: Allsopp, N., Colville, J.F., Verboom, G.A. (Eds.), Fynbos: ecology, evolution, and conservation of a megadiverse region. Oxford University Press, Oxford, pp. 142–163.

Tolley, K.A., Conradie, W., Pietersen, D.W., Weeber, J., Burger, M., Alexander, G.J. 2022 (In press). The Conservation Status of the Reptiles of South Africa, Eswatini and Lesotho. Publication volume xxxx. South African National Biodiversity Institute. Pretoria.

Townsend, T.M., Alegre, R.E., Kelley, S.T., Wiens, J.J., Reeder, T.W., 2008. Rapid development of multiple nuclear loci for phylogenetic analysis using genomic resources: an example from squamate reptiles. Mol. Phylogenet. Evol. 47 (1), 129–142.

Uetz, P., Freed, P., Aguilar, R., Hošek, J. (Eds.) (2022). The Reptile Database. Retrieved from http://www.reptile-database.org, accessed March 10, 2022.

Vaidya, G., Lohman, D.J., Meier, R., 2011. SequenceMatrix: concatenation software for the fast assembly of multi-gene datasets with character set and codon information. Cladistics 27 (2), 171–180.

Van Rossum, G., Drake, F. L., Jr., 1995. Python reference manual. Centrum voor Wiskunde en. Informatica, Amsterdam.

Van Zinderen Bakker, E.M., Mercer, J.H., 1986. Major late Cainozoic climatic events and palaeoenvironmental changes in Africa viewed in a worldwide context. Palaeogeogr. Palaeoclimatol. Palaeoecol. 56 (3–4), 217–235.

Vanden Broeck, A., et al., 2014. High levels of effective long-distance dispersal may blur ecotypic divergence in a rare terrestrial orchid. BMC Ecol. 14 (1), 1–15.

Verdcourt, B., 1969. The arid corridor between the north-east and south-west areas of Africa Palaeogeography. Palaeoclimatology, Palaeoecology 4 (1969), 140–144.

Voorhies, M.R., Holman, J.A., Xiang-Xu, X., 1987. The Hottell Ranch rhino quarries (basal Ogallala; medial Barstovian), Banner County, Nebraska; Part I; Geologic setting, faunal lists, lower vertebrates. Rocky Mt Geol. 25 (1), 55–69.

Wagner, P., Broadley, D.G., Bauer, A.M., 2012. A new acontine skink from Zambia (Scincidae: *Acontias* Cuvier, 1817). J. Herpetol. 46 (4), 494–502.

Warnes, G.R., et al., 2013. gplots: Various R programming tools for plotting data. R package version 2.12. 1. http://CRAN. R-project. org/package= gplots, last accessed March, 17, 2017.

Weinell, J.L., Bauer, A.M., 2018. Systematics and phylogeography of the widely distributed African skink Trachylepis varia species complex. Mol. Phylogenet. Evol. 120, 103–117.

Weinell, J.L., Branch, W.R., Colston, T.J., Jackman, T.R., Kuhn, A., Conradie, W., Bauer, A.M., 2019. A species-level phylogeny of *Trachylepis* (Scincidae: Mabuyinae) provides insight into their reproductive mode evolution. Mol. Phylogenet. Evol. 136, 183–195.

Whiting, A.S., Bauer, A.M., Sites Jr, J.W., 2003. Phylogenetic relationships and limb loss in sub-Saharan African scincine lizards (Squamata: Scincidae). Mol. Phylogenet. Evol. 29 (3), 582–598.

Wickham, H., 2017. tidyverse: Easily Install and Load "Tidyverse" Packages. URL https://CRAN. R-project. org/package= tidyverse. R package version, 1(1), 51.

Wiens, J.J., 2007. Species delimitation: new approaches for discovering diversity. Syst. Biol. 56 (6), 875–878.

Williams, K.J., et al., 2011. Forests of East Australia: The 35th Biodiversity Hotspot. In: Zachos, F., Habel, J. (Eds.), Biodiversity Hotspots. Springer, Berlin, Heidelberg.

Xia, X., 2017. DAMBE6: new tools for microbial genomics, phylogenetics, and molecular evolution. J. Hered. 108 (4), 431–437.

Yang, W., et al., 2020. Spatial variation in gene flow across a hybrid zone reveals causes of reproductive isolation and asymmetric introgression in wall lizards. Evolution 74 (11), 1289–1300.

Yu, Y., Blair, C., He, X., 2020. RASP 4: ancestral state reconstruction tool for multiple genes and characters. Mol. Biol. Evol. 37 (2), 604–606.

Zachos, J., Pagani, M., Sloan, L., Thomas, E., Billups, K., 2001. Trends, rhythms, and aberrations in global climate 65 Ma to present. Science 292 (5517), 686–693.

Zhang, D., et al., 2019. "Ghost introgression" as a cause of deep mitochondrial divergence in a bird species complex. Mol. Biol. Evol. 36 (11), 2375–2386.

Zhao, Z., Verdú-Ricoy, J., Mohlakoana, S., Jordaan, A., Conradie, W., Heideman, N., 2019. Unexpected phylogenetic relationships within the world's largest limbless skink species (*Acontias plumbeus*) highlight the need for a review of the taxonomic status of *Acontias poecilus*. J. Zool. Syst. Evol. Res. 57 (2), 445–460.

Zhao, Z., Heideman, N., Bester, P., Jordaan, A., Hofmeyr, M.D., 2020a. Climatic and topographic changes since the Miocene influenced the diversification and biogeography of the tent tortoise (*Psammobates tentorius*) species complex in Southern Africa. BMC Evol. Biol. 20 (1), 1–33.

Zhao, Z., Heideman, N., Grobler, P., Jordaan, A., Bester, P., Hofmeyr, M.D., 2020b. Unraveling the diversification and systematic puzzle of the highly polymorphic *Psammobates tentorius* (Bell, 1828) complex (Reptilia: Testudinidae) through phylogenetic analyses and species delimitation approaches. J. Zool. Syst. Evol. Res. 58 (1), 308–326.

Zheng, Y., Wiens, J.J., 2016. Combining phylogenomic and supermatrix approaches, and a time-calibrated phylogeny for squamate reptiles (lizards and snakes) based on 52 genes and 4162 species. Mol. Phylogenet. Evol. 94, 537–547.